This is to certify that the

thesis entitled

WATER QUALITY ASSESSMENT OF THE CHILUNG RIVER USING LANDSAT THEMATIC MAPPER AND AIRBORNE MULTI-SPECTRAL SCANNER IMAGES: TAIPEI, TAIWAN

presented by

Kin Man Ma

has been accepted towards fulfillment
of the requirements for

Masters of Science degree in Resource Development

Major professor

Date 11-25-97

WATER QUALITY ASSESSMENT OF THE CHILUNG RIVER USING LANDSAT THEMATIC MAPPER AND AIRBORNE MULTI-SPECTRAL SCANNER IMAGES: TAIPEI, TAIWAN

By

Kin Man Ma

A THESIS

Submitted to
Michigan State University
in partial fulfillment of the requirements
for the degree of

MASTERS OF SCIENCE

Department of Resource Development

1997

ABSTRACT

WATER QUALITY ASSESSMENT OF THE CHILUNG RIVER USING LANDSAT THEMATIC MAPPER AND AIRBORNE MULTI-SPECTRAL SCANNER IMAGES: TAIPEI, TAIWAN

By

Kin Man Ma

Due to the rapid, economic growth of Taiwan and the lack of effective wastewater treatment, Taiwan rivers, such as the Chilung River, have become polluted with increases in suspended sediments and biological oxygen demand, and decreases in dissolved oxygen. The Taiwan EPA field teams collected suspended sediments concentration (SSC) water quality samples. Remotely sensed image reflectance values have been correlated with SSC.

Three multi-temporal Landsat TM images from 1993 to 1995 and an April 1996 Airborne MSS image of the Chilung River were obtained. Landsat TM image reflectance values were normalized, transformed into radiance values, and regressed against monthly SSC data. The Airborne MSS image was geometrically resampled using ground control points and reflectance values were regressed against SSC and turbidity values.

Regression analyses yielded significant correlations between SSC and Landsat TM Band 4, $R^2 = 0.44$, $p = 0.009$. Natural log(SSC) and TM Band 4 correlation was more significant, $R^2 = 0.57$, $p = 0.002$. Band ratios generated significant correlations between ln(SSC) and the (Band 4/Band 2) ratio, $R^2 = 0.66$, $p < 0.001$.

Regression results between Airborne MSS Bands 8 and 9, and SSC levels yielded R^2 of 0.38 and 0.37, both $p = 0.001$. The turbidity and ln(turbidity) regressions against Airborne MSS Band 8 yielded similar results, $R^2 = 0.38$, $p = 0.001$.

This thesis is dedicated to my parents, Ding Fun Ma and Lai Yung Lam Ma, who have continually encouraged and supported me in my life and studies so that I could complete my Masters degree.

謹以本論文獻給我父親 馬鼎勳及母親 林麗容。感謝他們在我生活和學業上的支持鼓勵及三十年來對我毫無保留的付出，使我得以順利完成這個學位。

ACKNOWLEDGEMENTS

While conducting this international research project for my thesis, there were numerous people, organizations and institutions who have greatly assisted me and provided support for the completion of this work, both in Taiwan and in the Michigan State University (MSU) community.

Very significant assistance was received from the following people and groups in Taiwan:

I am very indebted to the Taiwan (Republic of China) Environmental Protection Administration (Project No.: EPA-85-L105-03-20) for the opportunity to participate in the foregoing research project from September 1995 to June 1996 and for funding this project conducted by the research team at the Center for Geographic Information Systems Research at Feng Chia University (FCU GIS Center). I thank the Taiwan EPA for their vision to improve the Taiwan environment through research.

Dr. Tien-Yin (Jimmy) Chou, Director of the FCU GIS Center, and a former graduate of the Department of Resource Development, was instrumental in fulfilling my desire to conduct research in East Asia. I joined the FCU GIS Center research team to work as a research assistant on the Taiwan EPA project and learned more about Asia and Taiwan as an exchange student through the MSU—FCU research exchange agreement. I am very thankful that he provided the data images for my thesis. I am also grateful to many of the research assistants, fellow

graduate students and staff for their academic and social support and encouragement, since I was the international student adjusting to a new culture. Thanks especially to Hui-Yen (Liz) Chen who worked on the project research team, guided me through many technical aspects of the research, and helped me understand scientific materials written in Chinese. Mei-Ling (Milly) Yeh, a fellow graduate student, was very understanding and supportive of my intellectual curiosity and showed me the joy of learning. Additional thanks to the FCU GIS Center for their financial support while my wife and I lived in Taichung.

Dr. Lung-Shih Yang, Dean of the College of Management, Feng Chia University (FCU), was the principal investigator of the Taiwan EPA project and he was supportive of my research efforts and was the first one to teach me about remote sensing.

Dr. Shanshin Ton, associate professor of environmental engineering, FCU, was the environmental engineer on our research team. He has been very encouraging and open to sharing his expertise in water related research in person and over E-mail.

Mrs. Agnes Chen, Director of the Mandarin Chinese Language Center, FCU, and other teachers challenged and encouraged my study of the Chinese language so that I could be a more effective researcher in Taiwan.

The following people and organizations in the MSU community provided significant assistance:

Travel to Taiwan was made possible in part through funding from the Department of Resource Development and the Institute for International Agriculture.

My Masters thesis committee members, Drs. Eckhart Dersch, Jon Bartholic, and Michael Kamrin, have been a tremendous source of wisdom and support during my thesis, especially my advisor, Dr. Dersch:

Dr. Eckhart Dersch, Professor of Resource Development, Michigan State University (MSU), has been overwhelmingly supportive through every step of my research journey from Michigan to Taiwan. He helped me establish connections with Dr. Jimmy Chou at FCU and he challenged me intellectually about development issues as well as thinking and acting proactively.

Dr. Jon Bartholic, Professor of Resource Development, Director of the Institute of Water Research, MSU, has challenged me to think critically about water research.

Dr. Michael Kamrin, Professor of Resource Development, Outreach Coordinator, Institute for Environmental Toxicology (IET), in 1994, gave me an opportunity to be a research assistant in IET and has continually endeavored to support my academic pursuits. He has challenged me intellectually and has been a role model for taking complex research ideas and concepts, digesting them and effectively explaining them to the general public.

The staff of IET, Carole Abel, Darla Conley, and Carol Chvojka, have been a tremendous encouragement and help throughout the years. IET has been a very stimulating environment for my intellectual growth regarding environmental issues with the intellectual prowess of Dr. William Cooper and a fellow graduate student, Jon MacDonagh-Dumler.

Dr. Cynthia Fridgen, Chair of the Department of Resource Development, has been very encouraging and supportive of my research since 1994.

Recognition needs to be given to the Geography Department, MSU, for allowing me to conduct my image data analysis on their computers. The following people provided significant assistance:

Dr. René Hinojosa, Chair of the Department of Geography, was supportive of multi-disciplinary connections and allowed me to use the UNIX computers for my research.

Dr. Daniel Brown, Assistant Professor of Geography, MSU, taught me about GIS. His advice about image reflectance and the use of the UNIX computers in the Spatial Analysis Laboratory for analyzing the Chilung River images have been invaluable.

Mr. James Brown, UNIX System Administrator, also assisted in UNIX account maintenance and answered questions regarding the Lab computers.

Jiunn-Der (Geoffrey) Duh, a fellow geography Ph.D. student, has taught me much about remote sensing and Taiwan. He was also very helpful to assist me in writing the Chinese dedication to my parents.

The following people also provided additional significant assistance:

Dr. David Lusch, Senior Research Specialist, Center for Remote Sensing and Geographic Information Science, MSU, has taught me the details and wonders of satellite remote sensing. He has been very helpful with critical analysis of my research methods and evaluation of my thesis.

Dr. Patricia Norris, Assistant Professor of Agricultural Economics and Resource Development, MSU, gave me an opportunity to use my GIS skills on her research project in Barry County. I have learned how to work hard and have been challenged to think about the economic implications of land use.

I also would not have completed this thesis without the following large network of spiritually and emotionally supportive friends, family, and the Lord God Almighty:

Miss Alexandra Saddler and Dr. Jennifer DeLapp have been long-time friends who have encouraged me with prayers and challenged me to keep my spiritual perspective even when the challenges seemed overwhelming.

The people at my church, University Reformed Church, have been instrumental for keeping me sane during this long process. Pastor Tom Stark has consistently preached the Word of God challenging me to love and serve others whenever and wherever I am. Dr. Mark Whalon, Professor of Entomology, Interim Director of the Pesticide Research Center, MSU, has been faithful to provide spiritual support and academic encouragement. The Brinkman family, KiSoon Kim, Dr. David and Elaine Prestel, Dr. Leland and Joella Cogan were always concerned about my academic and spiritual welfare. There are many others, though they are too numerous to name here.

Thanks to Ralph and Utami Rahardja DiCosty, fellow graduate students, since we have had many opportunities to pray, encourage and rejoice with one another about our mutual challenges and triumphs.

I also cannot forget my long-time doctor friends, Drs. David and Sharon (Blanchard) Gunasti, who have been very supportive in every way.

The people from the West Taichung Conservative Baptist Church in Taiwan were crucial in helping me spiritually and emotionally during the stressful time of conducting research in Taiwan. Pastor Lin was encouraging as well as the JiaLe small group, consisting of the family of Sam, Annie, Ellen and Tina Yang and

others. They were extraordinary in welcoming my wife and I into their hearts and challenging us to seek the Lord so we could both survive and flourish during our Taiwan experience.

Graduate InterVarsity Christian Fellowship have been a very encouraging and intellectually challenging group of people. Thanks, especially to Randy Gabrielse, Amy Hirshman, Sally Gaff, Tom Johnson, Mike Pasquale, Michelle Mackey, Sandeep Rao, Ying-ying (Sabrina) Wu, JiaNing Lai, and Reji Varghese. I do not have the space to mention all the others.

Hyunsook Lee Ma, my wife, has been truly supportive through the entire process of journeying to Taiwan for research and data collection as well as the recent challenges of thesis writing. I am indebted to her for the enduring patience, love, joy and perseverance she has shown me ever since we met. I consider it an honor to call her my wife.

My parents, Ding Fun Ma and Lai Yung Lam Ma, and my brother, Tony Ma, have been supportive of my studies throughout my life.

It is now appropriate to save the greatest thanks for last. The Lord God Almighty, has been my ultimate spiritual support because He is my wisdom. He has given me peace, joy and perseverance when circumstances were beyond my control regarding the use of the Taiwan data images. His protection while traveling to Taiwan, Korea, Hong Kong, New York City and back to Michigan has been reassuring.

"To God be the Glory" .....for this thesis.

November 1997
East Lansing, Michigan

The Lord God Almighty can see remotely...

11 "If I say, `Surely the darkness will hide me
and the light become night around me,'
12 even the darkness will not be dark to you;
the night will shine like the day,
for darkness is as light to you.

13 For you created my inmost being;
you knit me together in my mother's womb.
14 I praise you because I am fearfully and wonderfully made;
your works are wonderful, I know that full well."

– Psalm 139: 11-14

TABLE OF CONTENTS

LIST OF TABLES

LIST OF FIGURES

LIST OF ABBREVIATIONS

BOD	Biological Oxygen Demand
CAMS	Calibrated Airborne Multi-Spectral Scanner
DGPS	Differential Global Positioning System
DN	Digital Number
DO	Dissolved Oxygen
GCPs	Ground Control Points
GPS	Global Positioning System
MSS	Multi-Spectral Scanner
nm	nanometer
ROC	Republic of China (official name of Taiwan)
ROC EPA	Republic of China's Environmental Protection Administration
SDD	Secchi Disk Depth
SSC	suspended sediments concentration (mg/L)
TM	Thematic Mapper
TM 2°	Taiwan's National Transverse Mercator 2° coordinate
μm	micrometer

CHAPTER I

INTRODUCTION

A. Background

Taiwan is located in eastern Asia about 130 km (80.6 miles) southeast of the southern province of Fujian of the People's Republic of China. Taiwan's official name is the Republic of China (ROC) (See Appendix A).

Taiwan's economic development and the growth of the chemical, manufacturing, and electronics industries over the past 30 years have produced many commodities for the world. However, the release of untreated industrial chemicals and heavy metals associated with the production of these commodities and the growth of untreated residential, livestock and municipal landfill leachate wastewater have caused an increase in biological oxygen demand, an increase in the amount of suspended solids concentration, and an increase in other environmental pollutants, such as nitrogen compounds and phosphorous compounds. All of these contributing factors have lowered the water quality of the Taiwan river systems (Republic of China, Environmental Protection Administration (ROC EPA), 1994a).

Out of Taiwan's twenty-one main rivers, 25% of the total surface area of those rivers are either polluted or badly polluted, and out of Taiwan's 29 secondary rivers, 22.7% of the total surface area of those rivers are either polluted or badly polluted (ROC EPA, 1994a). The different categories of river pollution are shown in Table 1.1 for the following four water quality parameters: dissolved oxygen (DO),

biological oxygen demand (BOD), suspended sediments concentration (SSC), and ammonia nitrogen (NH_3-N).

Table 1.1 – Taiwan Categories of River Pollution for Water Quality Parameters

	Categories of River Pollution			
Water Quality Parameter	**Unpolluted**	**Slightly Polluted**	**Polluted**	**Badly Polluted**
Dissolved Oxygen (DO), mg/L	> 6.5	4.6 ~ 6.5	2.0 ~ 4.5	< 2.0
Biological oxygen demand (BOD), mg/L	< 3.0	3.0 ~ 4.9	5.0 ~ 15	> 15.0
Suspended sediments concentration (SSC), mg/L	< 20	20 ~ 49	50 ~ 100	> 100
Ammonia nitrogen (NH_3-N), mg/L	< 0.5	0.5 ~ 0.9	1.0 ~ 3.0	> 3.0

Source: Adapted from ROC EPA (1994a), p. 115.

Table 1.2 – 1986 and 1993 Comparison of Untreated Wastewater Sources Flowing into the Chilung River

	Wastewater Sources		Units: Metric Tons of Water/ Day			
Year	**Residential**	**Industrial**	**Livestock**	**Municipal Landfill Leachate**	**Agricultural**	**Total Effluents**
1986[1]	54.67 (Metric Tons)	12.62	18.33	8.02	-- N/A --	93.64
	58.38% (percentage of total)	13.48%	19.57%	8.57%	-- N/A --	100.0%
1993[2]	139.78 (Metric Tons)	24.63	2.60	0.26	0.37	167.64
	83.38% (percentage of total)	14.69%	1.55%	0.16%	0.22%	100.0%

Sources: 1. ROC EPA, December 1989; 2. ROC EPA, June 1994.

Taipei City, the capital of the Republic of China, has grown steadily over the past 20 years. The 1993 population in Taipei City's Chilung River watershed was 1.89 million people and is projected to be 2.08 million people by the year 2001 (ROC EPA, 1994b). With population growth, there has been corresponding growth in the amount of untreated residential wastewater released into the Chilung River which flows through the city. The total amount of untreated residential and industrial wastewater has almost tripled from 1986 to 1993. Residential wastewater as a percentage of the total daily effluent load has increased tremendously from 58.4% to over 83% in only 7 years (see Table 1.2).

Nearly all of Taipei City's untreated residential sewage and industrial wastewater flows into the Chilung River causing oxygen depletion and changes in BOD, SSC, and NH3. Field research teams have commented abut the hydrogen sulfide smell and the bubbling of the water's surface while taking water quality samples (ROC EPA, 1994a). As of 1996, there were no signs of living fish species in the downstream region of the Chilung River. During high tide, some saltwater fish species from the Taiwan Strait have swum into the Chilung River via the saltwater undercurrents (see Appendix B).

B. Research Area

The Chilung River begins in the Ching Tong mountains in southern Taipei County and flows west through Chilung City and through Taipei City and then it joins with the Tanshui River at Guan Du. The Chilung River is approximately 87 km (53.9 miles) long and has a surface area of 501 sq. km (193.4 sq. mi.), and is 250 meters wide (820 feet) near the mouth of the Chilung River and as narrow as 50 meters (164 feet) near the NanHu bridge. The region of the Chilung River entering

Taipei at the NanHu Bridge receives the largest amount of pollutants and therefore the eastern section of the research study area begins from Taipei City's NanHu Bridge and extends westward toward the mouth of the Tanshui River (see Appendices B, C, D and E).

1. Channel Modifications and Wastewater Treatment

The slope of the Chilung River is relatively flat with slopes ranging from 1 meter/500 meters or 0.2% at the NanHu bridge on the eastern side of the research area to 1 meter/700 meters or 0.14% at the BaiLing Bridge on the western side of the research area (see Appendices C and D). The average slope of the entire Chilung River is about 1 meter/118 meters or 0.85%.

From about November 1991 to late 1993, there were two (2) large channel modifications of the Chilung River for 1) increasing the flow rate of the Chilung River to prevent flooding during the summer monsoon season, and 2) to more effectively transport the increasing amounts of untreated residential wastewater from Taipei City residents toward the Taiwan Strait (see Appendices B, C and D).

There is presently one primary wastewater treatment plant near the DaZhi Bridge which is treating approximately 5% of the residential wastewater from Taipei City (ROC EPA, 1996). Beginning in 1994, Taipei City began a plan to build a network of wastewater diversion pipes and another primary wastewater treatment plant near the mouth of the Tanshui River close to the Taiwan Strait. The pipes would extend west along the Chilung River toward the point where it flows into the Tanshui River and then to the mouth of the Tanshui River (see Appendix B). There the sewage wastewater and storm drainage water would undergo primary wastewater treatment and then be emitted about 100 meters offshore into the

Taiwan Strait (ROC EPA, 1994b). As of June 1996, the wastewater pipes have yet to be completely built because of engineering problems and miscalculations regarding the total amount of wastewater which would bypass the Chilung River and flow toward the wastewater treatment plant before exiting into the Taiwan Strait. If the Chilung River doesn't receive any wastewater from the Taipei City residents or storm drainage water, the total water volume of the river would decrease, and ironically the river's concentration of pollutants may even increase.

2. Suspended Sediments

The suspended solids concentration (SSC) in the water is a physical indicator of water quality (Dzurik, 1990). When the SSC in the water is high, there are more suspended solids in the water, whether soil, algae, residential or industrial waste. If the SSC is low, the water can be assumed to have less silt, clay and fragments of organic matter, which indicates in general, better water quality.

3. Turbidity

Turbidity levels are another physical measure of water quality. Turbid water decreases the transparency of the water body and this opacity can be measured by a Secchi Disk. A Secchi Disk is a plastic disk approximately 20 cm in diameter with four quadrants. The quadrants are alternately black and white. This disk is lowered gradually into the water body until the white quadrants are no longer visible. This depth is then recorded as the Secchi Disk Depth (SDD). The SDD is related to the sediment content within the water body. Another "measure of turbidity is the use of nephometric turbidity units (NTU), which is measured by the intensity of light which passes through a water sample."[1]

---

[1] James B. Campbell, Introduction to Remote Sensing, (The Guilford Press, New York, NY,

Water of high turbidity decreases the intensity of the light in a manner that can be related to sediment content. Therefore, as sediment concentration increases the water body ceases to act as a "dark" object, absorbing most of the solar radiation, but slowly becomes more and more of a "bright" object, reflecting increasing amounts of light (Campbell, 1987).

4. Remote Sensing

Remote sensing is defined by Campbell (1987) as "the science of deriving information about the earth's land and water areas from images acquired at a distance. It usually relies upon measurement of electromagnetic energy reflected or emitted from the feature of interest."[2] After the invention of the airplane remotely sensed photographs and images were taken flying over the areas of interest. Moreover, with the 1960's discovery of space exploration and satellite technology, the United States in 1972 launched the Landsat 1 (Land Satellite), one of the first earth-orbiting satellites designed specifically for observation of the earth's land areas.

Remotely sensed images record the "interaction of electromagnetic radiation with the earth's surface. Electromagnetic radiation comes from several sources, such as changes in energy levels of electrons, decay of radioactive substances and the thermal motion of atoms and molecules."[3] Nuclear reactions in the sun produce a full range of electromagnetic radiation from ultraviolet rays, wavelengths of 0.30 micrometers (μm) to far infrared wavelengths, 7.0 – 15.0 μm. However, the earth's atmosphere of water vapor, ozone, and carbon dioxide gases absorbs certain portions

---

1987), p. 408.
[2] Ibid., p. 2.
[3] Ibid., p. 21.

of the electromagnetic spectrum preventing some solar radiation from penetrating the earth. There are a series of important atmospheric windows in which solar radiation can be transmitted. Therefore, only certain electromagnetic wavelengths within the earth's atmospheric windows can be used for measuring solar radiation reflectance from the earth's landscape. e.g. visible light, and the near-infrared, mid-infrared, and far-infrared wavelengths (see Figure 1.1).

Since 1972 many satellites such as the Landsat 2, 3, 4, and 5 were launched during the late 1970's and early 1980's. The developers of the Landsat 5 Thematic Mapper ("TM") satellite system set the sensitivity for each of the bands at specific wavelength intervals for principal applications of water body penetration, delineating water bodies, and for soil moisture discrimination (see Table 1.3).

The Landsat 5 satellite orbits the earth at an altitude of 705 km (438 miles) in a near polar orbit at a 98.2° angle to the equator. The satellite crosses the equator on the north-to-south portion of each orbit at 9:45 AM local sun time. Each orbit takes approximately 99 minutes, with about 14.5 orbits a day. The earth rotates approximately 2,752 km (1,710 miles) during each orbital pass, therefore the satellite sensor passes over the same 185 km (115 miles) swath area every 16 days. All of the Landsat TM band numbers 1 to 7 have pixel resolution sizes of 30 meters (98.4 feet), except the thermal band number 6 which has a pixel resolution of 120 meters (393.6 feet) (see Table 2.1, page 15).

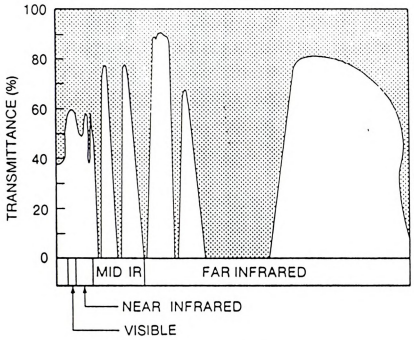

Atmospheric windows. This schematic representation can depict only a few of the most important windows. The shaded area represents absorption of electromagnetic radiation.

Figure 1.1 – Earth's Atmospheric Windows

Source: James B. Campbell, *Introduction to Remote Sensing*, (The Guilford Press, New York, NY, 1987), p. 34, Figure 2.9.

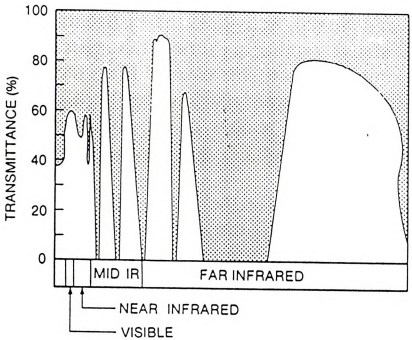

Atmospheric windows. This schematic representation can depict only a few of the most important windows. The shaded area represents absorption of electromagnetic radiation.

Figure 1.1 – Earth's Atmospheric Windows

Source: James B. Campbell, *Introduction to Remote Sensing*, (The Guilford Press, New York, NY, 1987), p. 34, Figure 2.9.

Table 1.3 – Landsat Thematic Mapper Spectral Bands

Band	Wavelength (μm)	Nominal Spectral Location	Principal Applications
1	0.45–0.52	Blue	Designed for water body penetration, making it useful for coastal water mapping. Also useful for soil/vegetation discrimination, forest type mapping, and cultural feature identification.
2	0.52–0.60	Green	Designed to measure green reflectance peak of vegetation (Figure 1.10) for vegetation discrimination and vigor assessment. Also useful for cultural feature identification.
3	0.63–0.69	Red	Designed to sense in a chlorophyll absorption region (Figure 1.10) aiding in plant species differentiation. Also useful for cultural feature identification.
4	0.76–0.90	Near infrared	Useful for determining vegetation types, vigor, and biomass content, for delineating water bodies, and for soil moisture discrimination.
5	1.55–1.75	Mid-infrared	Indicative of vegetation moisture content and soil moisture. Also useful for differentiation of snow from clouds.
6[a]	10.4–12.5	Thermal infrared	Useful in vegetation stress analysis, soil moisture discrimination, and thermal mapping applications.
7[a]	2.08–2.35	Mid-infrared	Useful for discrimination of mineral and rock types. Also sensitive to vegetation moisture content.

[a]Bands 6 and 7 are out of wavelength sequence because band 7 was added to the TM late in the original system design process.

Source: T.M. Lillesand and R.W. Kiefer, *Remote Sensing and Image Interpretation*, Third Edition, (John Wiley & Sons, Inc., New York, NY, 1994), p. 468, Table 6.4.

Airplane Airborne Sensors

There are other "portable" remote sensing sensors which are installed on airplanes and flown at altitudes between 5,000 to 10,000 feet. Flying at low altitudes reduces the amount of atmospheric scattering of solar light caused by gases and fine dust particles in the earth's atmosphere which affects satellite image reflectance. The spectral wavelengths intervals for the sensor's bands can be more narrowly set than those of the Landsat-5 TM sensor (see Table 2.1, page 15).

The spectral sensitivity of the Airborne Multi-Spectral Scanner (MSS) sensor bands can be calibrated to different ranges of wavelengths in order to accentuate the detection of certain earth phenomena. For example, the Airborne MSS sensor used for our research project has ten bands and the MSS Bands 3 to 6 are divided into 0.05 μm intervals. Please see Table 2.1 for the comparison of the Airborne MSS sensor with the Landsat TM sensor. A more detailed review of the MSS scanners band sensitivity will be found in Chapter 2.

C. Statement of the Problem

A review of the 1987 to 1995 average monthly water quality values for the Chilung River indicated that the river was polluted or badly polluted according to Taiwan's categories of river pollution (see Table 1.4 and compare with Table 1.1). Suspended sediment concentrations (SSC) ranged from a low of 2.0 mg/L at the BaiLing Bridge to a high of 424.0 mg/L at the DaZhi Bridge. Average monthly SSC values from 1987 to 1995 ranged from 35.0 mg/L to 78.4 mg/L. These SSC levels placed the Chilung River in the polluted category range of 50 — 100 mg/L (see Table 1.1). Average monthly biological oxygen demand (BOD) values ranged from a low of 9.0 mg/L to a high of 15.7 mg/L. These BOD values placed the Chilung River in the

polluted category range of 5.0 — 15.0 mg/L. Also, average monthly dissolved oxygen (DO) values ranged from a high of 4.2 mg/L to a low of 1.4 mg/L. These DO values placed the Chilung River in the polluted category range of 2.0—4.5 mg/L (see Table 1.1 and 1.4).

Table 1.4 – 1987 to 1995 Monthly Water Quality Parameter Averages of Chilung River Bridge Test sites (NanHu Bridge to BaiLing Bridge)

	Water Quality Parameter								
	SSC (mg/L)			BOD (mg/L)			DO (mg/L)		
Bridge Site	High	Low	Avg.	High	Low	Avg.	High	Low	Avg.
NanHu	226.0	5.0	51.0	36.0	1.6	13.8	7.6	0.0	2.7
ChengGong	132.0	5.0	35.0	28.0	2.7	11.9	7.7	0.8	4.2
ChengMai	249.0	4.0	50.2	29.0	2.4	10.4	8.4	0.3	3.8
MinQuan	236.0	23.0	78.4	21.8	3.3	9.0	8.1	0.7	3.1
DaZhi	424.0	11.0	61.7	37.0	0.9	14.0	8.1	0.0	3.0
ZhongShan	249.0	10.0	59.5	42.0	0.0	14.5	7.1	0.0	1.7
BaiLing	230.0	2.0	58.0	47.0	0.9	15.7	6.4	0.0	1.4

Source: Adapted from ROC EPA (1996), p. 31.

Presently, the Taiwan EPA sends out monthly water quality field collection teams on the Chilung River to gather water quality samples for analysis of parameters such as SSC, turbidity, biological oxygen demand and dissolved oxygen. The water quality data have been used by the Taiwan EPA and Taipei City officials for assessing the water quality status of the Chilung River and for establishing a water pollution control policy for Taipei.

However, the traditional water quality monitoring methods are costly, utilizing a large amount of economic and human resources. In addition, the water quality monitoring point samples cannot provide the synoptic view of the river

needed to help trace the sources of pollution. Remotely sensed images have been used for obtaining synoptic views of lakes, large rivers, and bay areas and also for analyzing the correlation between reflectance data values and water quality data (Alfoldi, 1982; Campbell, 1987; Curran et al., 1987; Rimmer et al., 1987; Lillesand and Kiefer, 1987, 1994; Welch et al., 1988; Braga et al., 1993, Mertes et al., 1993, Miller et al., 1994). It is not known whether the Chilung River, a small, shallow river, would be an appropriate site to test the use of remotely sensed images for monitoring the river's water quality.

D. Research Questions

Therefore, the objective of this study is to test whether the use of remotely sensed images will significantly correlate with water quality data and if so, determine whether a regular monitoring program for estimating a water quality parameter such as SSC can be developed using remotely sensed images such as Landsat Thematic Mapper (TM) images or Airborne Multi-Spectral Scanner (MSS) images. The following research questions narrow the focus of this study.

1) Can the water quality of the entire Chilung River be efficiently assessed using remotely sensed images and not just areas from which water quality point samples were collected?

2) Is there a significant correlation between the reflectance values of the remotely sensed images with the collected water quality data of the Chilung River?

3) Which type of remotely sensed images, Landsat TM or Airborne MSS, yield better correlations between Chilung River water quality values and their respective reflectance values?

This study was developed from the 1995-1996 Taiwan Environmental Protection Administration research project entitled, "The Application of Remote Sensing Technique to the Study of Environmental Pollution Monitoring" (Taiwan EPA-85-L105-03-20; ROC EPA, 1996). Dr. Lung-Shih Yang, Dean of the College of

Management, was the principal investigator joined by his colleague Dr. Tien-Yin Chou, both associate professors of Land Management at Feng Chia University (FCU) in Taichung, Taiwan. Dr. Chou is also the Director of the Center for Geographic Information Systems Research at FCU.

E. Organization

The remainder of the thesis has been organized according to the following chapters. Chapter 2 is the literature review of suspended sediments and remote sensing research. Chapter 3 details the research design and methodology for data analysis. Chapter 4 reviews the analysis of the Landsat TM and Airborne MSS data, correlation results, and discussion of the results. Chapter 5 includes the summary, conclusions, including answers to the research questions, and research recommendations.

F. Beneficiaries of the Research

The Taipei City and Taiwan federal government will better understand the effectiveness of using remotely sensed images to obtain a synoptic view of the Chilung River and aid in monitoring water quality parameters such as SSC and turbidity. They can then use this tool to devise and develop strategies to control and regulate industrial and residential effluents into the Chilung River.

Other countries may also benefit from this study by learning the utility of remotely sensed images for monitoring their own rivers. If this remote sensing technique produces significant correlations between water quality and image reflectance values, then other researchers can use Landsat TM and Airborne MSS images to correlate reflectance values in other rivers with water quality parameters such as suspended sediments concentration and turbidity.

CHAPTER II

LITERATURE REVIEW

A. Suspended Sediments

The interaction of light with a water-sediment mixture is complex because both materials scatter and absorb radiation. The total light reflectance (radiance) "measured remotely is not only a function of water and sediment properties, but also is a function of initial solar input, atmospheric transmission of the radiation, the upwelling radiance at the water surface and specular reflection off the water surface from both sunlight and skylight" (Mertes et al., 1993).

The "increase in the magnitude of the upwelling light affected by the concentration of suspended particles in the water is not linear because light is also absorbed by the water. As the amount of suspended particles increase, more light is reflected though portions of the path length of the light is also being absorbed. However, this increased reflectance is not a linear function. Those two interacting effects combine with the increased scattering with increased particle number resulting in a nonlinear increase in reflectance of water as sediment concentration increases" (Kirk, 1989).

In addition, as sediment concentration increases, spectral properties of the water change. First, the overall brightness in the visible region increases, so that the water begins to reflect more light, becoming more bright as sediment

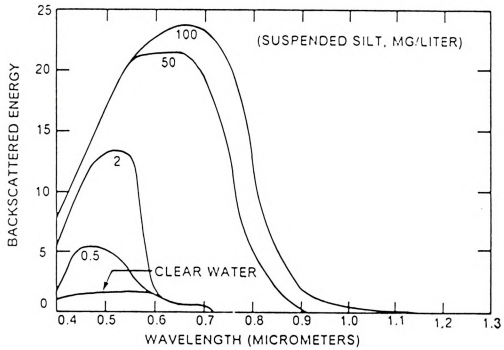

Figure 2.1 – Effects of Suspended Silt upon spectral properties of water.

Source: James B. Campbell, *Introduction to Remote Sensing*, (The Guilford Press, New York, NY, 1987), p. 408, Figure 14.5.

concentration increases. Secondly, as sediment concentration increases, the wavelength of peak reflectance shifts from the maximum in the blue-green region (0.4 to 0.5 micrometers), to the green region (0.5 to 0.6 μm) and then to the red (0.6 to 0.7 μm) and near infrared regions, 0.7 to 1.1 μm (see Figure 2.1). For the Landsat Thematic Mapper (TM) images, the red and near infrared regions correlates with Bands 3 and 4 (see Table 2.1).

B. Remote Sensing Research

Remote sensing image data such as the Landsat Multi-Spectral Scanner (MSS) and Thematic Mapper (TM) images have been used as effective tools to help evaluate aquatic resources. In Shimoda et al.'s (1986) Lake Balaton study, water quality monitoring of a Hungarian lake was studied using Landsat MSS data. Through regression analyses, transparency, suspended solids concentration, and chlorophyll-α content in Lake Balaton, were strongly correlated with the mean reflectance values of 3 x 3 pixel sections in the Landsat MSS image's Band #4, the near-infrared band, with a spectral sensitivity of 0.8 to 1.1 μm (Shimoda et al., 1986).

Other studies have utilized remotely sensed images to assess water quality parameters such as suspended solids concentration levels (SSC) and chlorophyll-α levels (Rimmer et al., 1987; Pattiaratchi et al., 1994). Pattiaratchi et al.'s (1994) research in Western Australia found that highly significant correlations for surface chlorophyll-α concentrations and Secchi Disk Depth (SDD), a measurement of water clarity, were obtained using Landsat TM Bands 1 and 3, 0.45 – 0.52 μm and 0.63 to 0.69 μm (see Table 2.1). A Secchi Disk is a plastic disk approximately 20 cm in diameter with four quadrants. The quadrants are alternately white and black. This

Table 2.1 – Comparison of Landsat TM and Airborne MSS Spectral Band Sensitivity

Spectral Sensit. (μm)	Spectral Location	Band No.	Band No.
		Landsat TM	Airborne MSS
0.38 – 0.42	Violet		1
0.42 – 0.45	Indigo		2
0.45 – 0.50	Blue	1 (0.45 -- 0.52 μm)	3
0.50 – 0.55	Green	2 (0.52 -- 0.60 μm)	4
0.55 – 0.60	Yellow	2 (0.52 -- 0.60 μm)	5
0.60 – 0.65	Orange	3 (0.63 -- 0.69 μm)	6
0.65 – 0.69	Red	3 (0.63 -- 0.69 μm)	7
0.70 – 0.79	Near Infrared	4 (0.76 -- 0.90 μm)	8
0.80 – 0.89	Near Infrared	4 (0.76 -- 0.90 μm)	9
0.92 – 1.10	Middle Infrared		10
1.55 -- 1.75	Middle Infrared	5	
2.08 -- 2.35	Middle Infrared	7	
10.40 -- 12.50	Thermal Infrared	6	
Image Resolution		30 meters (Bands 1 -- 5, and 7) 120 meters (Band 6 – Thermal)	5 meters (MSS Bands 1 – 10)

Adapted from: Lillesand and Kiefer (1994), p. 468 and ROC EPA (1996), p. 109.

disk is lowered into the water body until the white quadrants are no longer visible. This depth is then recorded as the SDD.

Rimmer et al. (1987) using Airborne Thematic Mapper data in Swansea Bay, United Kingdom correlated reflectance data with the water quality parameters, suspended solids concentrations and chlorophyll-α concentrations using linear and multiple regression analyses. Suspended solids concentrations were found to be most highly correlated with the blue/green and green portions, Bands 1 and 2 of the spectrum, 0.40 to 0.45 and 0.52 to 0.60 μm, though its radiance was affected by the size of the individual particles in suspension and their grain size distribution (Rimmer et al., 1987).

Curran et al. (1987) utilized an Airborne Multi-Spectral Scanner (MSS) image to estimate SSC along the Holderness coastline in England where there has been high rates of coastal erosion. According to Campbell's Figure 2.1, increasing SSC followed a logarithmic reflectance curve. Therefore, Curran et al. regressed the natural log (ln) of SSC and each of the Airborne MSS bands' radiance values. Airborne MSS band 7, 0.76 – 0.90 μm, generated the highest correlation, $R^2 = 0.46$, $p < 0.05$, while MSS band 8, 0.91 – 1.05 μm, also generated a similarly high correlation, $R^2 = 0.45$, $p < 0.05$. Other MSS bands 1 (0.42 – 0.45 μm), 4 (0.605 – 0.625 μm), and 5 (0.63 – 0.69 μm) generated similar correlations, $R^2 = 0.36$, $p < 0.05$ (Curran et al., 1987).

Khorram and Cheshire (1985) utilized Landsat MSS images to correlate turbidity and total suspended solids levels in the Neuse River Estuary, North Carolina. The ground resolution of the MSS was 80 meters, almost three times larger than Landsat Thematic Mapper's resolution of 30 meters. They generated a

complex band ratio multiple regression equation of MSS bands 4, 5, 6 and 7 for turbidity and this equation yielded, $R^2 = 0.76$, $p = 0.0004$. They also found a significant relationship between suspended solids and a complex band ratio of MSS bands 4, 5, 6 and 7 yielding an $R^2 = 0.64$, $p = 0.0001$ (Khorram and Cheshire, 1985).

The monitoring of suspended solids concentration have been effectively conducted in several foreign countries such as Brazil, Puerto Rico, and Australia. Braga et al. (1993) utilized Landsat TM images of the Guanabara Bay, Rio de Janeiro and through the correlation of TM bands, band ratios and principal component analysis (PCA), robust correlations of the suspended sediment concentrations with the Landsat-5 images of the Bay area were generated. Thematic Mapper Band 4 was the best band for the assessment of total suspended solids (TSS) with an $R^2 = 0.74$ for the regression equation (Braga et al., 1993).

Since Puerto Rico was located in a subtropical climate, Miller et al. (1994) used Calibrated Airborne Multi-Spectral Scanner (CAMS) images of the Mayagüez Bay in western Puerto Rico instead of Landsat-5 images because they could maintain greater control over the flight parameters to avoid interference from cloud cover. Estimates of low concentrations of suspended particles between 0 to 8 mg/L were highly correlated ($R^2 = 0.85$) to CAMS channel 4 reflectance, 0.63--0.69 micrometers (Miller et al., 1994).

In the Peel-Harvey Estuarine system of Western Australia, Lavery et al. (1993) utilized simple regression analyses to correlate channel water quality data with the Landsat TM band ratio values with water quality. Thematic Mapper bands 2 and 3 were significantly predictive of variations in Secchi Disk Depth, a measurement of water clarity (see Table 2.1).

CHAPTER III

RESEARCH DESIGN and METHODOLOGY

A. Water Quality Data

Before 1987, the Taipei City Environmental Affairs office monitored the water quality of the Chilung River, however, those records were inconsistent or inaccurate. After the formation of the Taiwan Environmental Protection Administration (Taiwan EPA) in 1987, there were regular monthly field tests of several environmental water quality factors such as the suspended sediments concentration (SSC), pH, turbidity and biological oxygen demand (BOD) on the Chilung River and the adjoining Tanshui River (see Appendices B, C and D). These monthly monitoring dates were not scheduled to coincide to the periodic flights of the Landsat-5 Thematic Mapper (TM) sensor over the Taipei, Taiwan region.

B. Landsat-5 Thematic Mapper satellite images

The studies reviewed in Chapter 2 have effectively used reflectance data from Landsat MSS and TM and Airborne MSS and TM images to evaluate the water quality of lakes, bays, estuaries and coastal water areas. Therefore, Landsat-5 TM images were selected for evaluating the correlation between the reflectance values and the suspended sediments concentrations and turbidity water quality parameters of the Chilung River. The Landsat-5 TM sensor flew over the Taipei,

Taiwan region at regular 16-day intervals (Lillesand and Kiefer, 1994, p. 463) and TM spectral bands 2, 3 and 4 (0.52 – 0.60 μm, 0.63 – 0.69 μm, and 0.76 – 0.90 μm) were sensitive to the different suspended sediment levels in the Chilung River (see Figure 2.1, page 15).

Landsat-5 TM satellite images were available from the National Central University's (NCU) Center for Space and Remote Sensing Research. They were selected to correspond temporally with Taiwan EPA's monthly water quality monitoring data of the Chilung and Tanshui Rivers from 1987 to 1995. The primary selection criteria for the TM images were: 1) no cloud cover over the two river bodies within the study area, 2) similar clear weather conditions, and 3) temporal proximity to the date(s) of the Taiwan EPA water quality monitoring data.

Three Landsat TM images were selected for correlation, Monday, June 28, 1993, Monday, January 9, 1995, and Monday, December 11, 1995 images, with the respective June 1993, January 1995, and December 1995 monthly water quality data. On June 27, 1993, the water quality field collection day, there was zero precipitation in Taipei. The records showed that there were 64 mm of rain on June 28, 1993, though this rain all fell in the afternoon after 9:45 AM (ROC National Weather Bureau, 1994), the normally scheduled time when the Landsat-5 TM sensor flew over Taipei and produced the first selected Landsat TM image (Lillesand and Kiefer, 1994, p. 462).

On January 6, 1995, there was zero precipitation in Taipei which is similar to the zero precipitation on January 9, 1995 when the second selected Landsat TM image was taken (ROC National Weather Bureau, 1995). And on December 7, 1995, there was zero precipitation in Taipei which is similar to the zero precipitation on

December 11, 1995, the date of the third selected Landsat TM image (ROC National Weather Bureau, 1996). According to the selection criteria, three selected images were the most closely matched to the corresponding water quality monitoring dates from 1987 to 1995.

1. Data Use and Analysis Limitations

Since the conclusion of the Taiwan EPA research project of the Chilung River (ROC EPA, 1996) conducted by the Center for Geographic Information Systems Research at Feng Chia University (FCU GIS Center) in June 1996, it was learned that the Landsat TM images and the Airborne Multi-Spectral Scanner image from the Taiwan EPA project could not be used outside of Taiwan because of national security and military reasons. However, in late March 1997, some additional negotiation resulted in permission to obtain color printed copies of the Landsat TM and Airborne MSS images, but only edited digital images for an area of the Chilung River water body with a land buffer of 200 meters along the river. Also, several 1:25,000 scale photogrammetric maps of the Taipei research area were obtained for locating bridge test sites on the Landsat TM and Airborne MSS images.

Therefore, with only edited images of the Chilung River water body, several of the water quality test sites from the adjoining Tanshui River were unable to be used for data analysis, reducing the total number of Landsat TM water quality data test sites from 22 to only 14 (see Table 3.1).

Table 3.1 – Water Quality Data and Landsat TM Band Reflectance Values

Testing Date	Image Date	Bridge Site	X_Coordin. Taiwan TM 2°	Y_Coordin. Taiwan TM 2°	SSC (mg/L)	Turbidity (NTU)	BOD (mg/L)	TM Band 1	TM Band 2	TM Band 3	TM Band 4
12/07/95	12/11/95	NanHu	310935.7	2773164.0	39.3	13	5.01	33	26	16	5
12/07/95	12/11/95	ChengMai	308017.2	2772042.4	97.3	11	6.46	35.5	29.5	22	5.5
12/07/95	12/11/95	MinChuan	306628.0	2773111.3	19.5	8	8.56	30	28	18	5
12/07/95	12/11/95	DaZhi	304131.4	2774554.5	27.5	10	7.45	37	29	21.5	3
12/07/95	12/11/95	ZhongShan	302140.3	2774265.1	18.0	11	9.88	34	28	18	5
12/07/95	12/11/95	BaiLing	300967.3	2775885.7	15.5	8	11.21	36	29	19.5	4.5
1/06/95	1/09/95	MinChuan	306581.7	2773165.3	52.0	62	8.72	43.5	32.5	29.5	8.5
1/06/95	1/09/95	DaZhi	304085.1	2774581.5	41.0	50	6.18	43	34	28.5	9
1/06/95	1/09/95	BaiLing	300944.1	2775908.9	81.0	45	7.79	44.5	32.5	28.5	9.5
6/27/93	6/28/93	ChengMai	308014.5	2772078.2	60.0	N/A	6.4	70	52.5	47.5	20.5
6/27/93	6/28/93	MinChuan	306580.9	2773138.9	103.0	N/A	6.0	69.5	55	50.5	23
6/27/93	6/28/93	DaZhi	304117.3	2774572.5	173.0	N/A	11.9	67.3	50.7	45	21
6/27/93	6/28/93	ZhongShan	302138.9	2774281.4	210.0	N/A	12.5	66	47.5	43.5	24
6/27/93	6/28/93	BaiLing	300972.5	2775903.3	203.0	N/A	8.3	68	48	43	22

Source: Modified from ROC EPA (1996), pp. 125-126.

2. Test Pixel Selection

Suspended solids concentration (SSC) was a visible indicator of water quality (Dzurik, 1990) and was selected for correlation analysis since this parameter has consistently been reported to have significant correlations with remotely sensed image reflectance data, such as Landsat TM image data (Shimoda et al., 1986; Rimmer et al., 1987; Ritchie et al., 1990; Braga et al., 1993; Lavery et al., 1993; Mertes et al., 1993; Han and Rundquist, 1994; Pattiaratchi et al., 1994; Liedtke et al., 1995). According to the Taiwan EPA's water quality data collection method, the field research team collected water quality samples between 10 to 30 meters upstream of each of the bridge sites while navigating up the middle of the Chilung River. The Landsat TM images have a spatial pixel resolution of 30 meters and the Landsat TM band reflectance values range from a low value of 0 to a high value of 255 which corresponds to the reflectance value of the target object (Lillesand and Kiefer, 1994). Therefore, each one of the test pixels was selected on average 30 to 60 meters, or 1 to 2 pixels upstream of the midpoint of the bridge monitoring sites. Pixels directly adjacent to the bridge test site were not selected in order to avoid obtaining a mixed pixel of combined reflectance values of the bridge site and the river water body. The reflectance values of the selected pixel and closest upstream neighbor pixel were averaged in order to decrease the chances of missing the true pixel position of the suspended sediment data reading. The bridge sites, water quality data readings, their respective position pixel(s) and corresponding band reflectance values were compiled in Table 3.1. All of the pixel coordinate positions were noted in Taiwan's Transverse Mercator 2° coordinate system.

3. Taiwan's Transverse Mercator 2° Coordinate System

Since Taiwan is only 140 km (84 miles) wide (ROC EPA, 1994a), the national government developed the Taiwan Transverse Mercator 2° (Taiwan TM 2°) local coordinate system to apportion the country into smaller and more precise sections than the Universal Transverse Mercator (UTM) 6° coordinate system. The false easting and false northing base coordinate points were positioned southwest of Taiwan and its regional islands at X = 250,000 and Y = 2,000,000 so that all coordinates throughout Taiwan and its regional islands have positive coordinate values.

4. Normalization of Landsat TM Reflectance Values

Since the three selected Landsat TM images of the ChiLung River were from different dates, the relative reflectance values on the images may differ from one image to another, because of differences in a) the seasons and b) the solar reflection angle, such as for the winter December 1995 and summer June 1993 images. Without normalization of the reflectance values, the comparison of spectral band values between the three images would be inaccurate. Therefore, normalization of the reflectance values for the three images were performed according to Jensen et al.'s (1995) method of multi-temporal image normalization.

5. Transformation from Reflectance Values to Radiance Values

When attempting to physically relate image data to quantitative ground measurements, especially for water resource evaluation, it is important to convert Digital Number (DN) reflectance values to absolute radiance values for each spectral band as shown in the formula below by Lillesand and Kiefer (1994).

Band Transformations to Radiance Values for mathematical modeling:

1) $DN = G*L + B$

$G*L = DN - B$

2) $L = \frac{DN - B}{G}$

DN = digital number value recorded

G = slope of response function (channel Gain)

L = spectral radiance measured (over the spectral bandwidth of the channel)

B = intercept of response function (channel Offset)

Source: Lillesand & Kiefer (1994), pp. 534-535.

Each of the spectral channel's gain and offset values were predetermined for the Landsat-5 TM satellite sensor. Each of the TM band's digital number reflectance values were calculated from the band's reflectance value multiplied by the gain value and adding its respective offset value (see Formula 1 above). Therefore, the TM band's digital number reflectance values were transformed to radiance values according to the image's offset and gain values utilizing Formula 2 above.

C. Airborne Multi-Spectral Scanner images

Airborne Multi-Spectral Scanner (MSS) sensors have been used by Curran et al. (1987) and Miller et al. (1994) for evaluating the correlation between the suspended sediments concentration (SSC) of the Holderness coastline in England and the Mayagüez Bay on the west coast of Puerto Rico, respectively. These Airborne MSS sensors can be mounted on airplanes and there are various sensors with different band spectral sensitivities that are used for specific research applications. Flying a small airplane with an Airborne MSS sensor allows researchers better scheduling control of the flight date and time. Taiwan's sub-tropical climate often produces rain which obscures solar radiation for taking good

images. Flying an Airborne MSS image would diminish the dependence upon the specific flyover date(s) of the periodic Landsat TM sensor.

Therefore, the Airborne MSS image was selected for evaluating the correlation between the reflectance values and the suspended sediments concentration and turbidity water quality parameters for the Chilung River. The Airborne MSS remotely sensed image provides improved ground pixel resolution (from 30 meters to 5 meters) and each spectral band's sensitivity is narrower than that of the Landsat Thematic Mapper (TM) sensor though it still covers the wavelengths at which SSC and turbidity reflect solar radiation (see Figure 2.1 and Table 2.1).

The Taiwan Provincial Government, Department of Forestry, Agroforestry Aerial Survey Division was contracted in November 1995 to fly over the Chilung River research area and photograph an Airborne MSS image. The flight had to be flown over Taipei on a clear day, though the winter months of December 1995 to March 1996 were the winter rainy season. Therefore, the Airborne MSS flight team was on daily stand-by waiting for a clear day to fly. The research team finally received notice from the Agroforestry Aerial Survey Division on Thursday, April 25, 1996 at 8:30 AM of a clear day, and the Airborne MSS flight was flown over the Chilung River. Immediate preparations were made to coordinate and dispatch the field collection team on Thursday night to prepare for the collection of the water quality samples on Friday, April 26, 1996 at about the same time of the Airborne MSS flight.

1. Differential Global Positioning System

In order to more accurately determine the position on the Airborne MSS image at which the water quality data was collected, the Differential Global

Positioning System (DGPS) was used. DGPS uses a reference receiver located at a known location to compute Global Positioning System (GPS) corrections for use by another remote receiver at an unknown position. In DGPS, the "reference (base) receiver compares its position solution it calculates with the true position coordinates of its location, in order to derive satellite-specific pseudorange corrections. These corrections are applicable within the local region and can be used to improve the position accuracy of the remote receiver which is obtaining positions of unknown locations" (Lusch, 1996). One study demonstrated that without differential processing in open terrain, root mean square errors (rmse) were 4.88 -- 6.95 meters but with differential processing, the accuracies were reduced to 1.30 -- 5.89 meters rmse (Lusch, 1996).

A Garmin 100 GPS base receiver was positioned at a known base reference point on the roof of the President Hotel, Taipei, Taiwan. The base station receiver continually received coordinate positions from at least four orbiting global positioning satellites. The other Garmin 100 receiver accompanied one of the field team members. At each data collection point, the team member turned on the receiver for at least 3 minutes to obtain at least 180 position readings (one per second).

2. Water Quality Data

For the first twenty-two water quality data points, the field collection team was successful in obtaining Differential Global Positioning System (DGPS) readings of the location of the water quality test site, but since the upstream region of the Chilung River east of the MinQuan Bridge was very shallow, the boat could not maneuver there. Therefore, a separate field collection team drove to the three upstream bridge sites, ChengMai, ChengGong, and NanHu, and took water quality

Table 3.2 – Water Quality Data and 4/25/96 Airborne MSS Reflectance Values

No.	Test Site	Date and Collection Time	X_Coordinate Taiwan TM 2°	Y_Coordinate Taiwan TM 2°	SSC (mg/L)	Turbidity (NTU)	BOD (mg/L)	MSS Band_1	MSS Band_2
		4/26/96						4/25/96	
1	ChiLung Mouth	11:03	296070.2	2778440.6	17.2	51	10.5	100	147
2	HaiZhuan	11:11	296761.9	2778296.5	10.6	53	9.6	112	167
3	XiaBaXian	11:22	297895.1	2778663.1	21.0	46	11.4	82	140
4	ZhongBaXian	11:29	298571.3	2778838.4	16.4	55	11.7	99	141
5	ShangBaXian	11:35	299048.0	2778565.6	29.2	56	11.4	63	129
6	BeiTou	11:43	299292.9	2777921.5	11.8	53	11.1	79	89
7	LiTaiShuiNi	11:50	299398.5	2776934.3	14.2	51	10.8	54	79
8	ShuangXi	12:00	300421.7	2776718.1	4.2	53	12.6	74	142
9	BaiLing Bridge	12:08	300982.5	2775910.5	11.4	59	13.7	83	134
10	HouGang	12:13	301233.2	2775002.8	16.6	60	12.3	131	152
11	ChengDe	12:24	301749.5	2774811.6	23.8	61	12.0	130	169
12	ZhongShan Bridge	12:33	302127.8	2774397.5	10.8	67	10.5	151	173
13	Highway #1	12:41	302429.4	2774469.4	13.3	68	9.3	69	128
14	ZhongShan Station	12:47	303013.1	2774626.1	45.6	69	9.2	168	147
15	DaZhi Bridge	12:57	303991.6	2774572.8	16.0	58	10.5	120	141
16	DaZhi Station	13:07	305148.3	2774446.2	28.0	55	8.7	113	150
17	Bian Bridge	13:14	305605.2	2774220.1	16.0	49	7.5	83	133
18	HuanKo Pump	13:20	306179.5	2774266.5	3.0	50	7.2	88	106
19	GangQian	13:29	306536.4	2774500.6	11.2	50	8.3	62	67
20	GangQian Station	13:35	306800.3	2774318.2	10.7	52	8.4	30	58
21	Highway #2	13:40	306869.9	2773858.5	8.2	55	8.4	48	63
22	MinQuan Bridge	13:50	306603.5	2773765.0	17.4	57	9.0	38	60
23	ChengMai Bridge	12:15	307987.7	2772034.0	81.1	99	6.0	142	148
24	ChengGong Bridge	11:50	308910.5	2772643.4	91.6	100	6.6	116	144
25	NanHu Bridge	11:30	310907.9	2773143.2	94.4	106	6.0	93	175
26	President Hotel	base point	302142.5	2773492.3					

Adapted from ROC EPA (1996) and modified by Kin M. Ma (1997)

Table 3.2 – (cont'd)

No.	Test Site	MSS Band_3	MSS Band_4	MSS Band_5	MSS Band_6	MSS Band_7	MSS Band_8	MSS Band_9	MSS Band_10
1	ChiLung Mouth	107	74	117	101	91	35	23	29
2	HaiZhuan	108	77	120	105	95	38	25	29
3	XiaBaXian	100	76	119	108	103	43	29	33
4	ZhongBaXian	95	74	119	108	103	45	31	34
5	ShangBaXian	86	85	107	96	94	41	28	34
6	BeiTou	63	48	76	68	65	28	18	22
7	LiTaiShuiNi	66	47	73	64	60	24	15	19
8	ShuangXi	101	72	111	103	102	46	31	31
9	BaiLing Bridge	103	76	117	106	100	41	26	31
10	HouGang	110	81	123	110	101	40	25	29
11	ChengDe	109	80	125	113	106	43	28	33
12	ZhongShan Bridge	116	85	131	119	110	44	28	32
13	Highway #1	104	79	124	116	109	44	27	29
14	ZhongShan Station	107	80	126	117	114	50	32	33
15	DaZhi Bridge	111	83	129	122	118	48	31	33
16	DaZhi Station	99	74	119	109	105	43	28	33
17	Bian Bridge	101	77	122	113	107	43	29	33
18	HuanKo Pump	71	55	89	83	80	32	21	25
19	GangQian	55	41	67	67	69	33	26	30
20	GangQian Station	43	33	54	50	48	20	13	15
21	Highway #2	59	44	72	66	63	26	17	20
22	MinQuan Bridge	46	34	55	51	48	20	13	16
23	ChengMai Bridge	105	78	126	114	107	42	26	30
24	ChengGong Bridge	114	81	133	128	127	55	36	36
25	NanHu Bridge	117	80	128	124	129	65	46	43

Adapted from ROC EPA (1996), pp. 71, 75, and 114

readings standing on the eastern side of each bridge midway across the span of the Chilung River (see Table 3.2). Water quality samples for testing the SSC, turbidity, and BOD parameters were taken by using 10 cm diameter cylinders, 30 to 40 cm in length. Each water sample was collected 100 cm below the river's surface. The 30 to 40 cm water column was thoroughly mixed and each of the cylinders were immediately iced and returned to Feng Chia University's Environmental Engineering laboratory the same day for chemical testing according to the standard water quality testing procedures for each parameter.

3. Image Correction and Resampling

The raw Airborne MSS image contained geometric distortions, because of variations in the altitude, the velocity of the sensor, the earth's curvature, and relief displacement and therefore could not be used as a map of the research area. When the Airborne MSS image was acquired from the National Central University's Center for Space and Remote Sensing Research, it was then geometrically corrected and resampled by finding twelve Ground Control Points (GCPs) such as large road intersections or the runways at the Sungshan Airport on 1:5,000 scale photogrammetric maps of the Taipei City area. These points were items in the landscape which were easily located on both the Airborne MSS image and on the maps. Then the Airborne MSS image was resampled into Taiwan's national TM 2° coordinate system in order to match Taiwan's maps using the nearest neighbor resampling method (Campbell, 1987; Lillesand and Kiefer, 1994).

4. Selection of Test Pixel Positions

The coordinate positioning data sets from each receiver were differentially processed by the FCU GIS Center research team in May 1996 to accurately determine the exact coordinate positions of the water quality data points and their respective pixel locations on the Airborne MSS image. The original positions data were not available, however, each of the Taiwan TM 2° X,Y coordinate positions of the water quality sites were provided in the ROC EPA (1996) Final Report, page 75 (see Table 3.2).

An edited Airborne MSS image of the Chilung River water body from the NanHu bridge to the mouth of the Chilung River with a land buffer of 200 meters adjacent to the river was also used for finding the water quality digital sampling sites. Therefore, analysis of the land features affecting the SSC was not possible. Each of the band's reflectance values at each of the water quality sampling sites on the Chilung River were then extracted from the Erdas Imagine imaging software program for data analysis as presented in Table 3.2.

Since there were three bridges above shallow water, the research boat could not reach them. The site nos. 23, 24, and 25 did not have DGPS readings. Therefore, the field team took water quality samples from the middle of the eastern side of the above bridge sites. During pixel selection, the length of the span of the eastern side of each bridge was measured and the pixel at the midpoint of the length was selected. Then the closest eastern pixel to the selected pixel not under the shadow of each bridge was chosen for the point of water quality data collection and all of the pixels' reflectance values were recorded (see Table 3.2).

D. Data Analysis Methodology

Previous studies have utilized linear and multi-linear regression analyses to show correlations between image reflectance data and SSCs (Khorram and Cheshire, 1985; Curran et al., 1987; Rimmer et al., 1987; Pattiaratchi et al., 1994; Liedtke et al., 1995) and turbidity (Shimoda et al., 1986). Linear and multiple-regression analyses were performed on the SSC water quality parameter, with the Landsat TM radiance and the Airborne MSS reflectance band values. Also, different band combinations of linear and multiple-regression analyses were performed to test the hypothesis that the various band ratios significantly correlate with the respective water quality parameters. Digitally corrected radiance values and the corresponding water quality parameters were correlated using linear and multi-linear regression analyses (Lavery et al., 1993; Miller et al., 1994).

Through multiple regression analysis, a relationship between the spectral radiance values and the corresponding SSC water quality data can be found. This relationship has been represented by the following model equation (Clark and Hosking, 1986; Rimmer et al., 1987):

$$Y = \beta_0 + \beta_1 X_1 + \beta_2 X_2 + ... + \beta_n X_n + \varepsilon$$

Y represents the water quality value
X_1, X_2, X_n represents the reflectance or radiance values of the spectral bands
$\beta_0, \beta_1, \beta_2, \beta_n$ represent the partial regression coefficients for each X independent variable
ε represents the residual factor

CHAPTER IV

DATA ANALYSIS, RESULTS and DISCUSSION

A. Landsat TM related data

1. Taiwan EPA Water Quality Data

a. Suspended Sediments

Among the three dates for the water quality readings, the lowest suspended sediments concentration (SSC) reading of 18.0 mg/L was at the ZhongShan bridge site on December 7, 1995. The highest SSC reading was 210 mg/L, also at the ZhongShan bridge site on June 27, 1993. The average SSC readings at the December 7, 1995 test sites were 36.2 mg/L, at the January 6, 1995 test sites, 58.0 mg/L, and for the June 27, 1993 test sites, 149.8 mg/L (see Figure 4.1).

The SSC values for the June 1993 data were significantly higher than the other two dates because beginning in November 1991, the Chilung River was undergoing a massive re-channeling project for almost two years. Dr. Shanshin Ton, the environmental engineer on the research team, examined the monthly SSC data from 1991 and 1993 and other engineering documents. He concluded that this significant engineering project caused considerable increase in sediment levels throughout the entire Chilung River during that period.

b. Turbidity

The turbidity level readings for the Chilung River have been included in Table 3.1 for reference, though since the turbidity bridge site readings from the June 1993 Taiwan EPA water quality data were not available, the remaining data set was extremely small, 9 data points, and therefore correlation analysis was not performed on the turbidity data. However, the correlation results for turbidity and the Airborne MSS image data will be summarized later in this chapter.

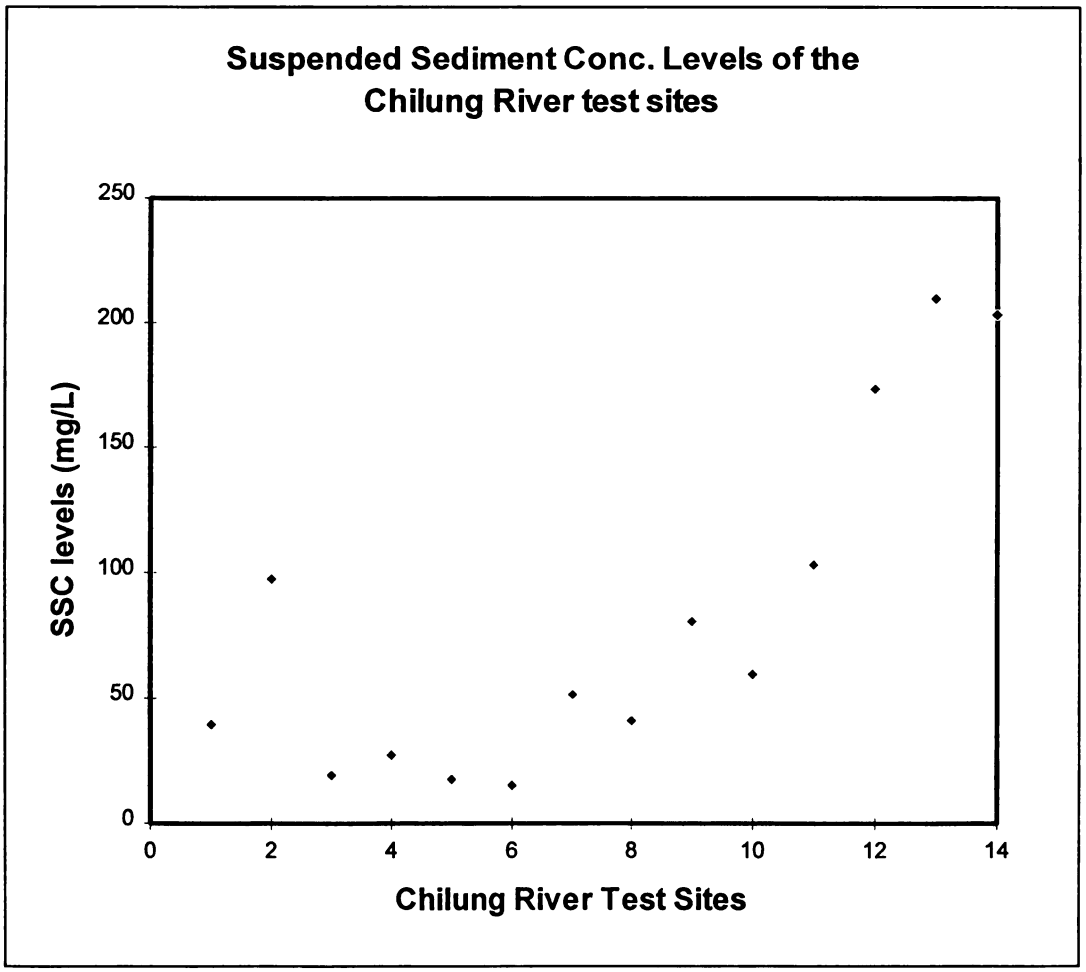

Figure 4.1 – Graph of the SSC levels of Chilung River bridge test sites.

The low numbered sites began from the December 1995 data and the higher numbered bridge sites are the June 1993 data points (see Table 3.1, page 23, for reference).

2. Landsat TM Images

After an initial observation of the Landsat TM reflectance values for Bands 5 and 7, the majority of the reflectance values for Band 5 (mid-infrared) were zero and the remaining values were all less than five. The reflectance values for Band 7 were almost all zero. Water is a very efficient absorber of light in the mid-infrared regions of the electromagnetic spectrum and therefore the reflectance values for Bands 5 and 7 were almost negligible and therefore eliminated from the data analysis.

As mentioned above in Chapter 3, only edited Landsat TM images of the Chilung River body were available for this study, so that extensive digital analysis of the Taipei land areas and their potential influences on the water quality of the Chilung River was not possible. Nevertheless, in order to perform accurate analysis of the spectral band's values between the images, the three Landsat TM images were normalized according to Jensen et al.'s (1995) method of multi-temporal image normalization.

a. Normalization of Landsat TM images

The normalization method was performed by the Feng Chia University GIS Center research team in April 1996 and the results were presented in the Taiwan EPA Final Report, "The Application of Remote Sensing Technique to the Study of Environmental Pollution Monitoring" (ROC EPA, 1996, pp. 103-107). The December 11, 1995 image was chosen as the base image and the two other images were normalized to the base image. For the normalization of the January 9, 1995 image, twelve ground control points (GCPs) were chosen having the following criteria with the aid of 1:5,000 scale photogrammetric maps: a) targets were in a relatively flat

area, and b) patterns on the normalization targets had not changed over the three-year period, from June 1993 to December 1995. Chosen GCPs included sites such as 1) golf courses, 2) cemeteries, and 3) landing strips of the SungShan airport in central Taipei. After the target points were selected on both images, the respective reflectance values for Bands 1 to 4 were noted. The two sets of values were regressed, designating the 12/11/95 values as the dependent variable and the 1/9/95 values as the independent variable. The linear regression equations and R^2 correlations for each of the Landsat TM bands 1 through 4 were generated as follows (see example Figures 4.2 to 4.3). For the image normalization of the 6/28/93 to the 12/11/95 image, ten (10) GCPs were chosen having the same criteria as stated above (see example Figures 4.4 to 4.5).

Each of the test site values from the January 1995 and June 1993 images were normalized to the December 11, 1995 Landsat TM images by inserting their respective reflectance values as the X value in the following regression equations:

Normalization of 1/09/95 values to the 12/11/95 values:
1/09/95 Normalized_TM Band#1 = (0.911197 * 1/9/95 TM Band#1) - 0.22207
1/09/95 Normalized_TM Band#2 = (1.08021 * 1/9/95 TM Band#2) - 1.53298
1/09/95 Normalized_TM Band#3 = (0.971503 * 1/9/95 TM Band#3) - 2.66149
1/09/95 Normalized_TM Band#4 = (0.663747 * 1/9/95 TM Band#4) + 6.35655

Normalization of 6/28/93 values to the 12/11/95 values:
6/28/93 Normalized_TM Band#1 = (0.565355 * 6/28/93 TM Band#1) - 0.0830209
6/28/93 Normalized_TM Band#2 = (0.736734 * 6/28/93 TM Band#2) - 5.95241
6/28/93 Normalized_TM Band#3 = (0.725341 * 6/28/93 TM Band#3) - 9.21851
6/28/93 Normalized_TM Band#4 = (0.421847 * 6/28/93 TM Band#4) + 3.87658

The results of the normalization of Landsat TM bands for the 1/09/95 and 6/28/93 images are tabulated in Tables 4.1 and 4.2.

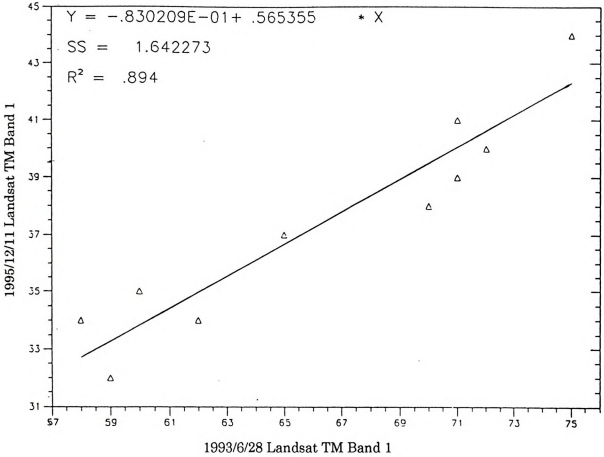

Figure 4.4 – Landsat TM images, 6/28/93 to 12/11/95 normalized regression graph (TM Band 1).

Source: ROC EPA, *The Application of Remote Sensing Technique on the Study of Environmental Pollution Monitoring.* Prepared by the Center for Geographic Information Systems Research, Feng Chia University, June 1996, Taichung, Taiwan, 163 pp., (in Chinese), p. 106.

Table 4.1 – Landsat TM Bands 1 to 4 values, Normalized from the 1/09/95 image to the 12/11/95 image

Image Date	Bridge Site	TM Band#1	TM Band#2	TM Band#3	TM Band#4	Normalized Band#1	Normalized Band#2	Normalized Band#3	Normalized Band#4
1/09/95	MinChuan	43.5	32.5	29.5	8.5	39.4150	33.5738	25.9978	11.9984
1/09/95	DaZhi	43	34	28.5	9	38.9594	35.1942	25.0263	12.3303
1/09/95	BaiLing	44.5	32.5	28.5	9.5	40.3262	33.5738	25.0263	12.6621

Table by Kin M. Ma (1997)

Table 4.2 – Landsat TM Bands 1 to 4 values, Normalized from the 6/28/93 image to the 12/11/95 image

Image Date	Bridge Site	TM Band#1	TM Band#2	TM Band#3	TM Band#4	Normalized Band#1	Normalized Band#2	Normalized Band#3	Normalized Band#4
6/28/93	ChengMai	70	52.5	47.5	20.5	39.4918	32.7261	25.2352	12.5244
6/28/93	MinChuan	69.5	55	50.5	23	39.2092	34.5680	27.4112	13.5791
6/28/93	DaZhi	67.3	50.7	45	21	37.9654	31.4000	23.4218	12.7354
6/28/93	ZhongShan	66	47.5	43.5	24	37.2304	29.0425	22.3338	14.0009
6/28/93	BaiLing	68	48	43	22	38.3611	29.4108	21.9712	13.1572

Table by Kin M. Ma (1997)

b. Transformation from Reflectance Values to Radiance Values

The Landsat TM normalized reflectance values were then transformed into radiance values according to Formula 2 mentioned in Chapter 3.

$$2) \qquad L = \frac{DN - B}{G}$$

DN = digital number value recorded
G = slope of response function (channel Gain)
L = spectral radiance measured (over the spectral bandwidth of the channel)
B = intercept of response function (channel Offset)

Source: Lillesand & Kiefer (1994), pp. 534-535.

The Gain and Offset values for each of the Landsat 5 Thematic Mapper bands for data processed in Taiwan are listed below:

	Gain	**B (Offset)**
Landsat TM #1	1.659939989	2.523108752
Landsat TM #2	0.850992808	2.416819498
Landsat TM #3	1.241057044	1.452036688
Landsat TM #4	1.227673274	1.853786631

Source: ROC EPA (1996), p. 102.

The results of the transformed Landsat TM radiance values for all three images and their four TM bands are shown in Table 4.3.

Table 4.3 – Landsat TM Normalized and Transformed Band Radiance Values

Image Date	Bridge Site	SSC (mg/L)	ln (SSC)	Norm. TM Band 1	Norm. TM Band 2	Norm. TM Band 3	Norm. TM Band 4	Transform. TM Band 1	Transform. TM Band 2	Transform. TM Band 3	Transform. TM Band 4
12/11/95	NanHu	39.3	3.6712	33	26	16	5	18.3602	27.7125	11.7222	2.5627
12/11/95	ChengMai	97.3	4.5778	35.5	29.5	22	5.5	19.8663	31.8254	16.5568	2.9700
12/11/95	MinChuan	19.5	2.9704	30	28	18	5	16.5529	30.0627	13.3338	2.5627
12/11/95	DaZhi	27.5	3.3142	37	29	21.5	3	20.7700	31.2378	16.1539	0.9336
12/11/95	ZhongShan	18	2.8904	34	28	18	5	18.9627	30.0627	13.3338	2.5627
12/11/95	BaiLing	15.5	2.7408	36	29	19.5	4.5	20.1675	31.2378	14.5424	2.1555
1/09/95	MinChuan	52	3.9512	39.415	33.574	25.998	11.998	22.2248	36.6126	19.7781	8.2633
1/09/95	DaZhi	41	3.7136	38.959	35.194	25.026	12.330	21.9504	38.5166	18.9953	8.5336
1/09/95	BaiLing	81	4.3944	40.326	33.574	25.026	12.662	22.7738	36.6126	18.9953	8.8039
6/28/93	ChengMai	60	4.0943	39.492	32.726	25.235	12.524	22.2711	35.6164	19.1636	8.6918
6/28/93	MinChuan	103	4.6347	39.209	34.568	27.411	13.579	22.1008	37.7807	20.9170	9.5508
6/28/93	DaZhi	173	5.1533	37.965	31.400	23.422	12.735	21.3515	34.0581	17.7025	8.8636
6/28/93	ZhongShan	210	5.3471	37.230	29.042	22.334	14.001	20.9088	31.2877	16.8258	9.8944
6/28/93	BaiLing	203	5.3132	38.361	29.411	21.971	13.157	21.5899	31.7206	16.5336	9.2072

Table by Kin M. Ma (1997), adapted from Tables 3.1, 4.1, and 4.2.

Table 4.4 – Landsat Thematic Mapper Data Regression Results

Water Quality Parameter	Thematic Mapper Band and Band Combinations	R^2	F- test	*p* *(p < 0.001)
SSC	Band 1	0.137	1.905	0.193
SSC	Band 2	0.006	0.068	0.799
SSC	Band 3	0.094	1.246	0.286
SSC	**Band 4 10.611 * (Band 4) - 17.844**	**** 0.444**	**9.599**	**0.009**
SSC	**Band 4/Band 2**	**** 0.575**	**16.238**	**0.002**
SSC	**Band 4/Band 3**	**** 0.560**	**15.255**	**0.002**
SSC	ln (Band 4)	0.389	7.633	0.017
SSC	ln (Band 4/Band 3)	0.406	8.189	0.014
SSC	ln (Band 4/Band 2)	0.443	9.554	0.009
SSC	**Band 2, Band 3, Band 4**	**** 0.844**	**18.054**	***** 0.001**
ln (SSC)	Band 2	0.065	0.761	0.402
ln (SSC)	Band 3	0.271	4.081	0.068
ln (SSC)	**Band 4**	**** 0.574**	**16.176**	**0.002**
ln (SSC)	**(Band 4/Band 2)**	**** 0.658**	**23.055**	***** 0.001**
ln (SSC)	**(Band 4/Band 3)**	**** 0.629**	**20.332**	**0.001**
ln (SSC)	(Band 3/Band 4)	0.268	4.389	0.058
ln (SSC)	(Band 2/Band 4)	0.335	6.046	0.030
ln (SSC)	ln (Band 1)	0.279	4.641	0.052
ln (SSC)	ln (Band 2)	0.086	1.134	0.308
ln (SSC)	ln (Band 3)	0.268	4.393	0.058
ln (SSC)	**ln (Band 4)**	**** 0.518**	**12.878**	**0.004**
ln (SSC)	**ln (Band 4/Band 3)**	**** 0.492**	**11.618**	**0.005**
ln (SSC)	**ln (Band 4/Band 2)**	**** 0.551**	**14.704**	**0.002**
ln (SSC)	**ln (Band 2), ln (Band 3), ln (Band 4)** **- 14.105 * (ln B#2) + 7.575 * (ln B #3) + 0.893 (ln B#4) + 30.714**	**** 0.851**	**19.002**	***** 0.001**

** yielded relatively high R^2 values

Table by Kin M. Ma (1997)

Table 4.4 – Landsat Thematic Mapper Data Regression Results

Water Quality Parameter	Thematic Mapper Band and Band Combinations	R^2	F- test	*p* *(p < 0.001)
SSC	Band 1	0.137	1.905	0.193
SSC	Band 2	0.006	0.068	0.799
SSC	Band 3	0.094	1.246	0.286
SSC	**Band 4** **10.611 * (Band 4) - 17.844**	**** 0.444**	**9.599**	**0.009**
SSC	**Band 4/Band 2**	**** 0.575**	**16.238**	**0.002**
SSC	**Band 4/Band 3**	**** 0.560**	**15.255**	**0.002**
SSC	ln (Band 4)	0.389	7.633	0.017
SSC	ln (Band 4/Band 3)	0.406	8.189	0.014
SSC	ln (Band 4/Band 2)	0.443	9.554	0.009
SSC	**Band 2, Band 3, Band 4**	**** 0.844**	**18.054**	*** 0.001**
ln (SSC)	Band 2	0.065	0.761	0.402
ln (SSC)	Band 3	0.271	4.081	0.068
ln (SSC)	**Band 4**	**** 0.574**	**16.176**	**0.002**
ln (SSC)	**(Band 4/Band 2)**	**** 0.658**	**23.055**	*** 0.001**
ln (SSC)	**(Band 4/Band 3)**	**** 0.629**	**20.332**	**0.001**
ln (SSC)	(Band 3/Band 4)	0.268	4.389	0.058
ln (SSC)	(Band 2/Band 4)	0.335	6.046	0.030
ln (SSC)	ln (Band 1)	0.279	4.641	0.052
ln (SSC)	ln (Band 2)	0.086	1.134	0.308
ln (SSC)	ln (Band 3)	0.268	4.393	0.058
ln (SSC)	**ln (Band 4)**	**** 0.518**	**12.878**	**0.004**
ln (SSC)	**ln (Band 4/Band 3)**	**** 0.492**	**11.618**	**0.005**
ln (SSC)	**ln (Band 4/Band 2)**	**** 0.551**	**14.704**	**0.002**
ln (SSC)	**ln (Band 2), ln (Band 3), ln (Band 4)** **- 14.105 * (ln B#2) + 7.575 * (ln B #3) + 0.893 (ln B#4) + 30.714**	**** 0.851**	**19.002**	*** 0.001**

** yielded relatively high R^2 values

Table by Kin M. Ma (1997)

c. Linear Regression Analysis and Results

Each of the four normalized and transformed radiance band values were regressed against the SSC values. The regression of SSC and TM Band 4, 0.76 - 0.90 μm, yielded the only significant correlational relationship (R^2 = 0.444, p = 0.009) (see Table 4.4 and Figure 4.6). Campbell (1987) and Kirk (1989) have shown that the relationship between SSC and spectral radiance has a logarithmic relationship at increasingly higher SSC concentrations (see Figure 2.1, page 15). Therefore, additional regression analyses were performed between the natural log (ln) of the dependent variable, SSC, and the other independent band variables. As shown in Table 4.4, the regression of the ln(SSC) dependent variable and the Band 4 radiance values yielded the highest significant single band correlational relationship (R^2 = 0.574, p = 0.002) with a regression equation: ln(SSC) = 0.157*(Band 4) + 2.582. The graph for this correlation is in Figure 4.7.

In addition, Braga et al. (1993) performed regression analyses on band ratio combinations. Since increasing amounts of sediment in the water will shift the amount of reflected energy to the longer visible and near-infrared wavelengths, there may be a relationship with the Infrared/Red, Band 4/Band 2 and Band 4/ Band 3 combinations. The regression of SSC with the Band 4/Band 2 band ratio yielded R^2 = 0.575, p = 0.002 and the Band 4/ Band 3 band ratio yielded R^2 = 0.560, p = 0.002. When ratio band regression relationships were tested with ln(SSC), the logarithmic relationships also yielded significantly high R^2 values. For example, the regression of the ln(SSC) variable and the (Band 4/Band 2) ratio yielded R^2 = 0.658, $p < 0.001$ (see Table 4.4 and Figure 4.8) and the regression of ln(SSC) variable and

the (Band 4/Band 3) ratio yielded $R^2 = 0.629$, $p = 0.001$ with the following regression equations:

$$\ln(SSC) = 7.440 * (\text{Band 4/Band 2}) + 2.723;$$

$$\ln(SSC) = 4.049 * (\text{Band 4/Band 3}) + 2.465.$$

When the log/log function relationship was tested, ln(SSC) and ln(Band 4/Band 2) yielded $R^2 = 0.551$, $p = 0.002$.

d. Multiple Regression Analysis and Results

When multiple regression analyses were computed the Log/Log relationship between ln(SSC) and the ln(Band2), ln(Band3), ln(Band4) band combinations yielded the highest $R^2 = 0.851$, $p < 0.001$ in the following multiple regression equation:

$$\ln(SSC) = -- 14.105*(\ln \text{Band\_2}) + 7.575*(\ln \text{Band\_3}) + 0.893*(\ln \text{Band\_4}) + 30.714$$

When the Landsat TM 2, 3 and 4 band combination were regressed against SSC, it yielded a significant correlation of $R^2 = 0.844$ and $p < 0.001$ with the following regression equation:

$$SSC = --31.109 *(\text{Band\_2}) + 23.983 *(\text{Band\_3}) + 19.423 *(\text{Band\_4}) + 592.721.$$

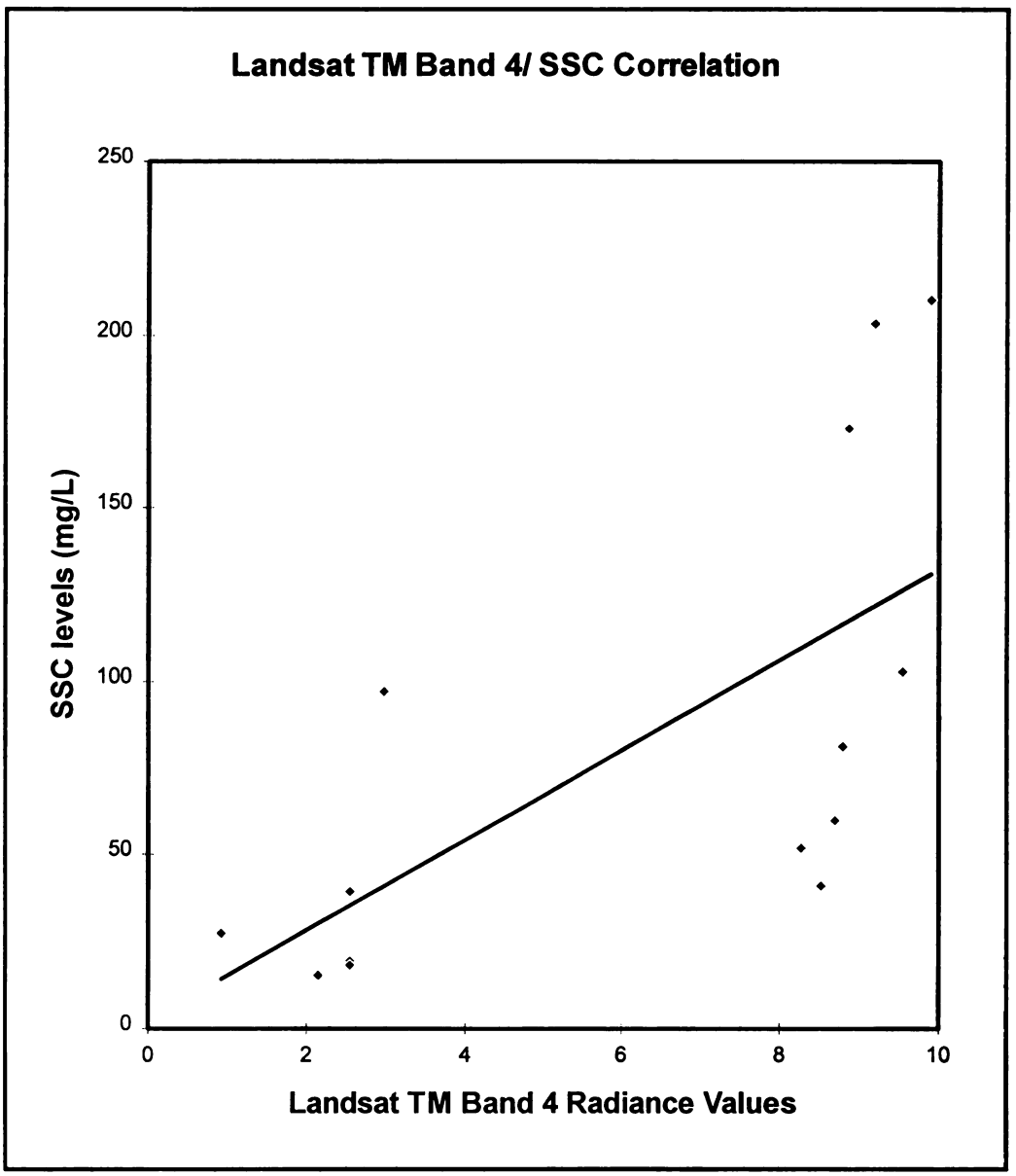

$R^2 = 0.444$, $p = 0.009$

SSC = 10.611 * (Band_4) -- 17.844

Figure 4.6 – Graph of Correlation between Landsat TM Band 4 and SSC.

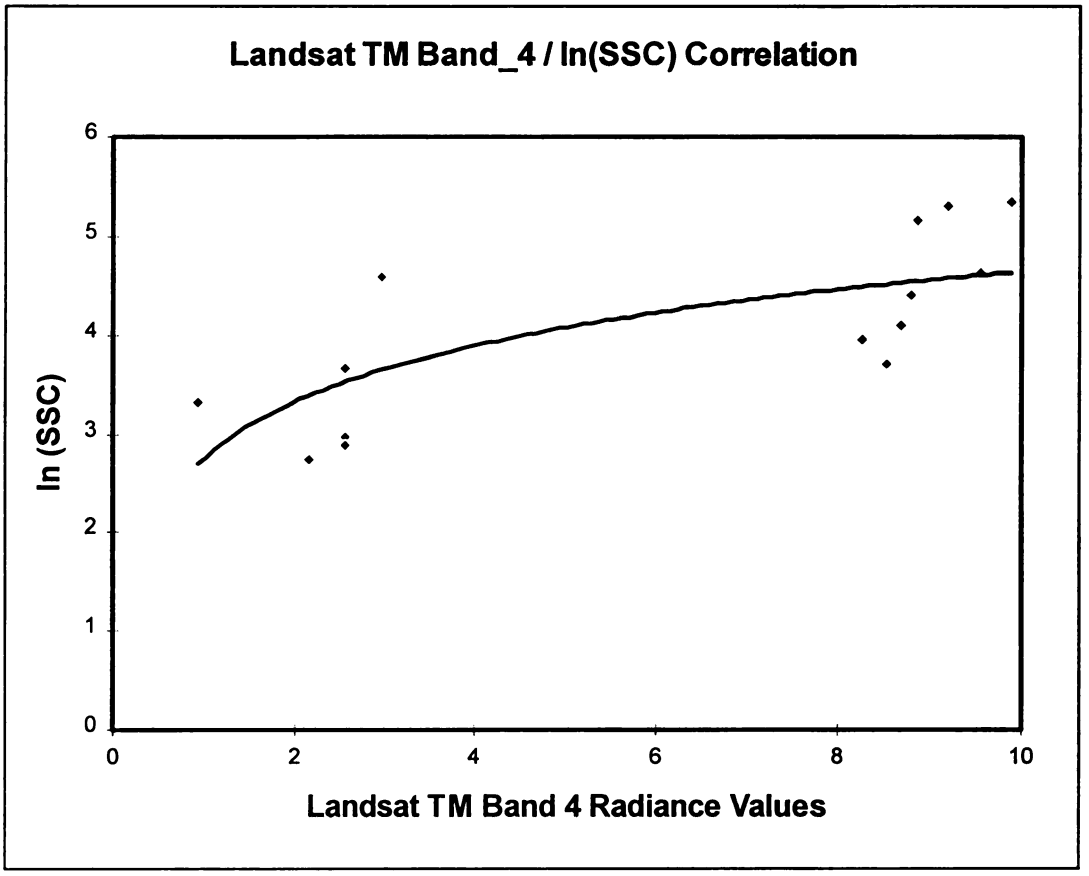

$R^2 = 0.574$, $p = 0.002$

ln (SSC) = 0.157 * (TM Band_4) + 2.582

Figure 4.7 – Graph of Correlation between Landsat TM Band 4 and ln(SSC).

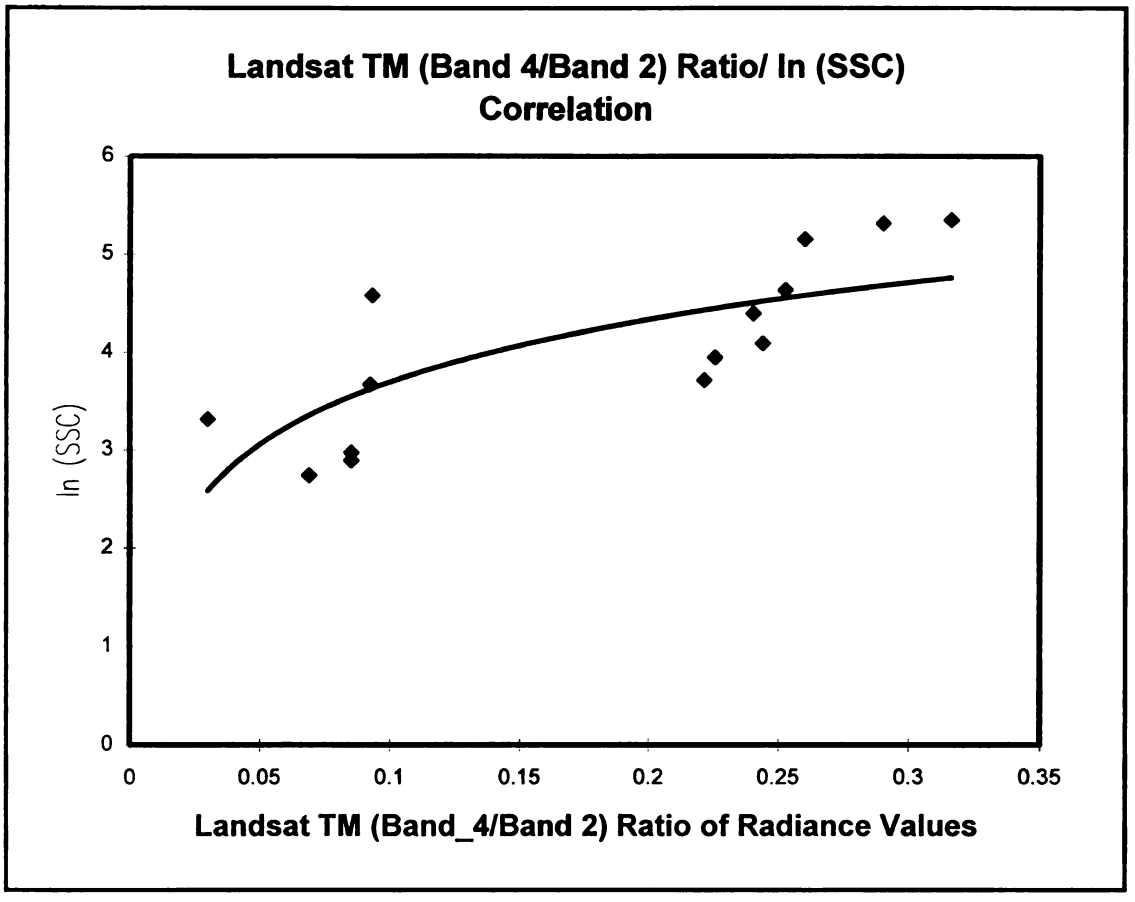

$R^2 = 0.658$, $p < 0.001$

ln (SSC) = 7.440 * (TM Band_4/TM Band_2) + 2.723

Figure 4.8 – Graph of Correlation between Landsat TM (Band 4/Band 2) Ratio and ln(SSC).

B. Airborne MSS related data

1. Water Quality Data

a. Suspended Sediments

All of the water quality data were from the April 26, 1996 field collection day. The SSC values for the test points showed that the water quality of the Chilung River was slightly polluted to polluted according to Taiwan's water quality standards in Table 1.1, page 2, with an average SSC value of 24.9 mg/L, a high value of 94.4 mg/L and a low value of 3.0 mg/L. The average of the BOD values was 9.7 mg/L, with a high value of 13.7 mg/L and a low value of 6.0 mg/L. The average BOD values places it in the "polluted" rivers category, 5.0 – 15.0 mg/L, as shown in Table 1.1, page 2.

The SSC readings at the last three sites, Nos. 23, 24, and 25, were especially high, averaging 89.0 mg/L, because the river is very shallow, only 2 meters deep, east of the MinQuan Bridge and it may have been influenced by the ongoing nearby construction on the Taipei highway (see Figure 4.9).

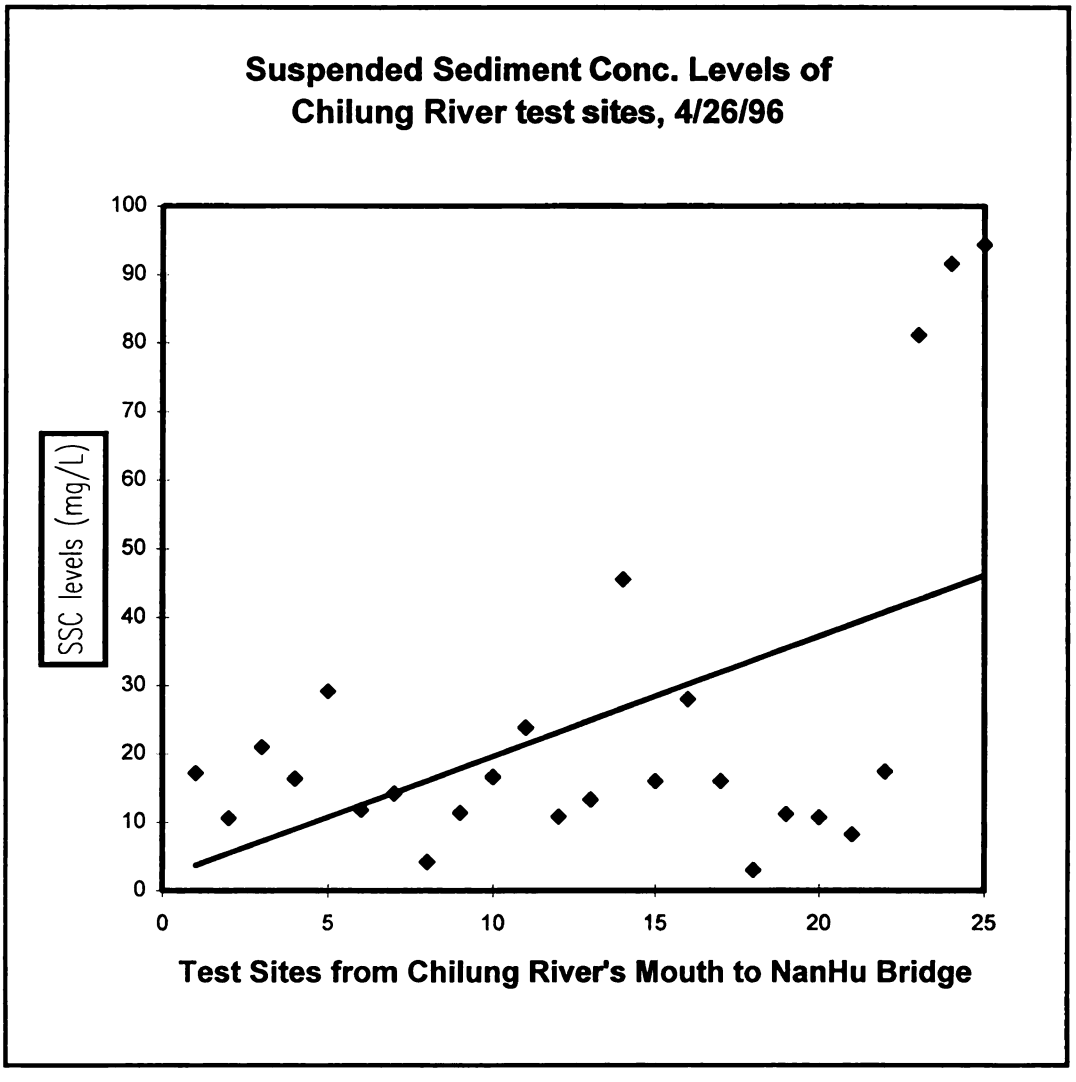

Figure 4.9 – Graph of the SSC levels of Chilung River test sites, 4/26/96.

The test sites begin from the mouth of the Chilung River and the site numbers increase going eastwards along the Chilung River toward the NanHu Bridge (see Table 3.2, page 29 for reference).

b. Turbidity

Also, the average of the turbidity values was 61.3 NTU, with a high value of 106 NTU and a low value of 46 NTU. The turbidity readings at the last three sites, Nos. 23, 24, and 25, were especially high, averaging 101.6 NTU, because the river was very shallow, only 2 meters deep, east of the MinQuan Bridge and it may have been influenced by the ongoing nearby construction on the Taipei highway (see Figure 4.10). Turbidity levels are highly significantly correlated with SSC values, $R^2 = 0.855$, F-test 136.11, $p \leq 0.001$ (see Figure 4.11).

2. Regression Analysis and Results

a. Suspended Sediments

Linear regression analyses of Airborne MSS Bands 1 to 5 and SSC did not yield any significant correlational relationships, at a 95% confidence level. All of the regression analyses of the Airborne MSS Bands 6 to 10 were significant ($p \leq 0.05$). The linear regressions of SSC and MSS Bands 8 and 9 yielded the strongest correlations, $R^2 = 0.377$, $p = 0.001$, and $R^2 = 0.366$, $p = 0.001$, respectively (see Table 4.5 and Figure 4.12).

Logarithmic combinations were also tested and again correlations with MSS Bands 6 to 10 were significant though they were not as highly correlated as the above MSS Band 8 correlation. For example, when ln(SSC) was regressed against MSS Band 8, $R^2=0.305$, $p = 0.004$ (see Figure 4.13).

Many band ratio regressions were also tested such as the MSS Band 9/Band 7 (Infrared Red/Red) ratio though almost all of the correlation results were not significant at the 95% confidence level, and therefore not included in the results.

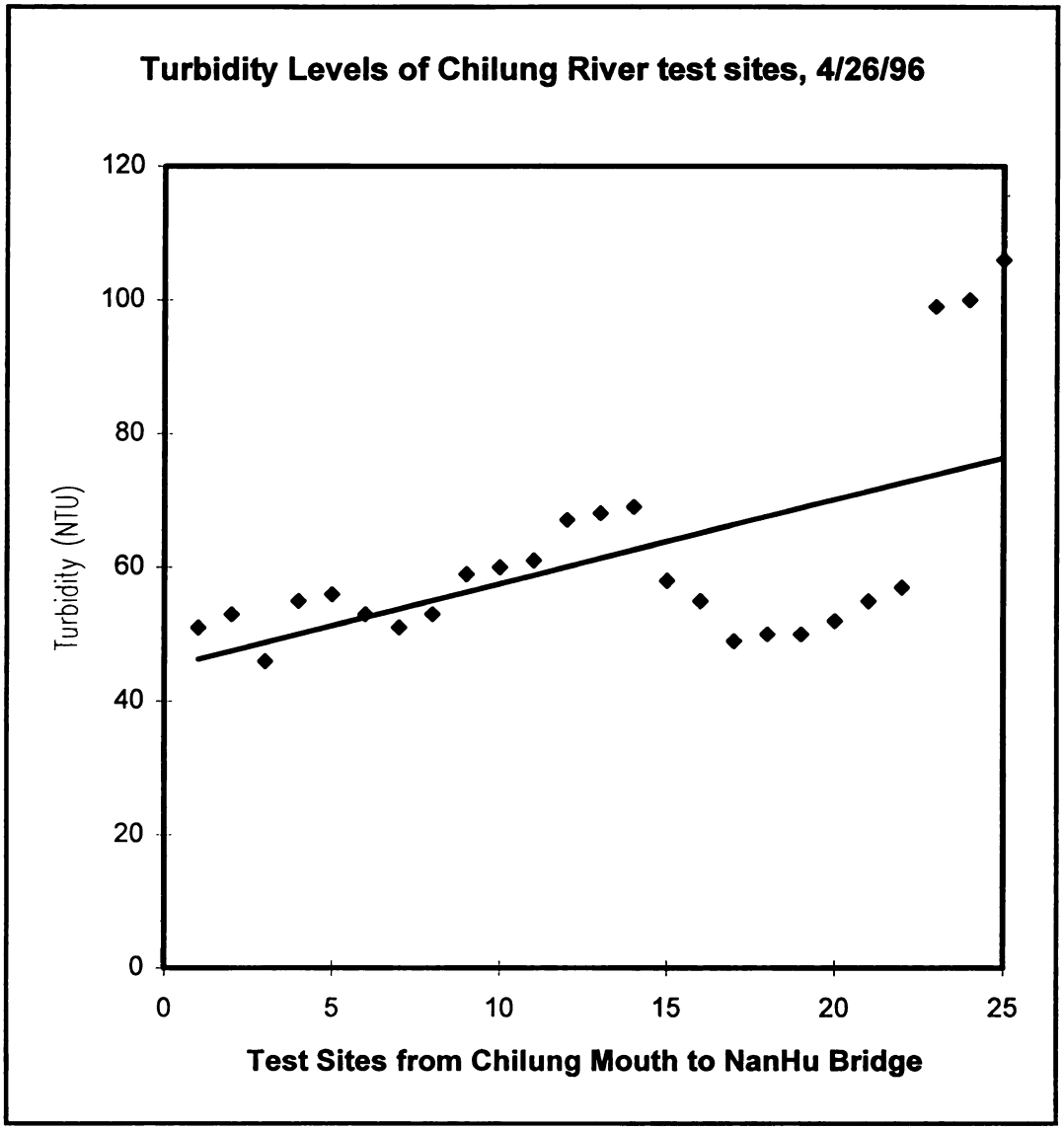

Figure 4.10—Graph of the Turbidity levels of Chilung River test sites, 4/26/96.

The test sites begin from the mouth of the Chilung River and the site numbers increase going eastwards,along the Chilung River toward the NanHu Bridge (see Table 3.2, page 29 for reference).

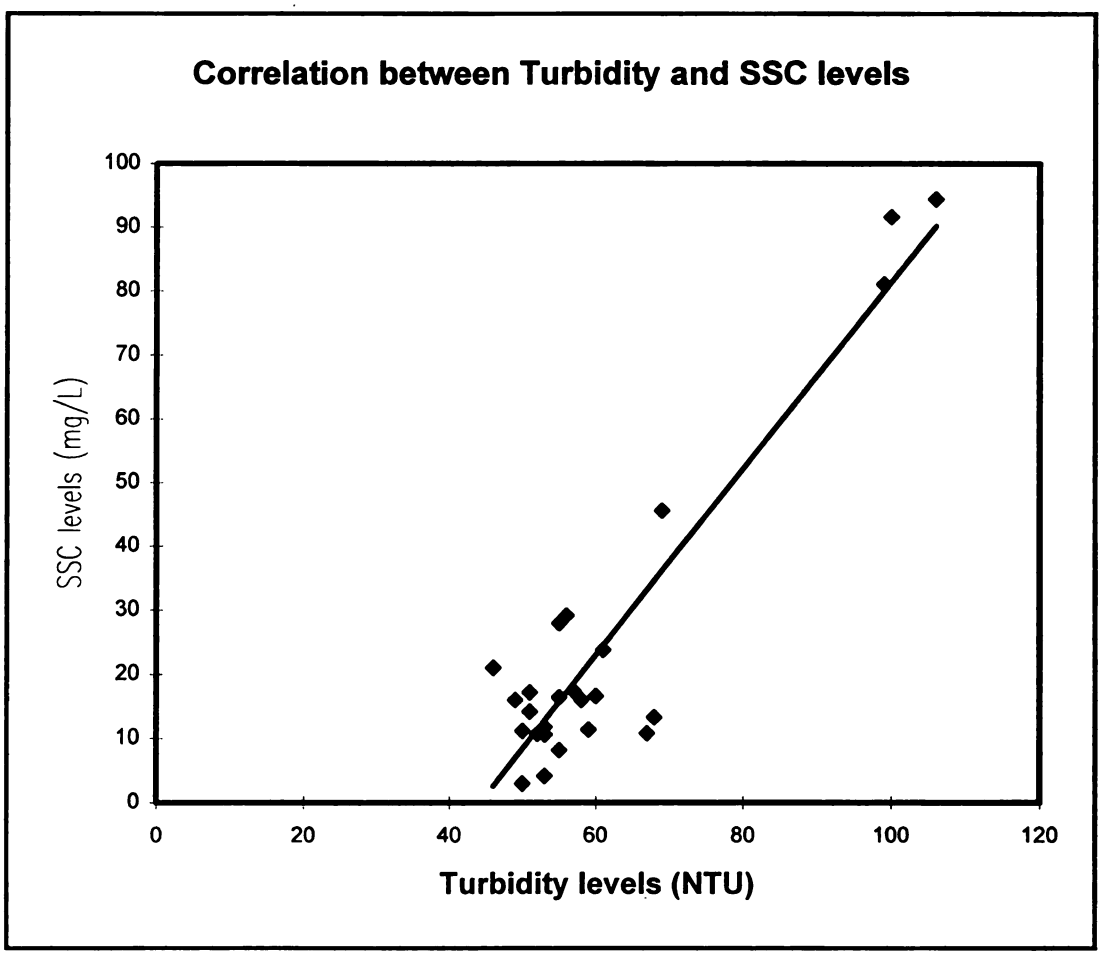

$R^2 = 0.855$, F-test 136.11, $p \leq 0.001$

Figure 4.11 – Graph of Correlation between Turbidity values and SSC values.

Table 4.5 – Airborne Multi-Spectral Scanner Data Regression Results

Water Quality Parameter	Airborne MSS Band and Band Combinations	R^2	F- test	*p* *(p < 0.001)
SSC	Band 1	0.137	3.655	0.068
SSC	Band 2	0.143	3.838	0.062
SSC	Band 3	0.164	4.499	0.045
SSC	Band 4	0.128	3.375	0.079
SSC	Band 5	0.170	4.696	0.041
SSC	Band 6	0.216	6.332	0.019
SSC	Band 7	0.284	9.105	0.006
SSC	**Band 8** **1.495 * (MSS Band_8) – 34.197**	**** 0.377**	**13.910**	**0.001**
SSC	**Band 9**	**** 0.366**	**13.261**	**0.001**
SSC	Band 10	0.269	8.453	0.008
SSC	ln (Band 6)	0.173	4.828	0.038
SSC	ln (Band 7)	0.215	6.309	0.019
SSC	ln (Band 8)	0.274	8.667	0.007
SSC	ln (Band 9)	0.261	8.103	0.009
SSC	ln (Band 10)	0.199	5.717	0.025
ln (SSC)	Band 1	0.164	4.515	0.045
ln (SSC)	Band 2	0.154	4.183	0.052
ln (SSC)	Band 3	0.176	4.910	0.037
ln (SSC)	Band 4	0.171	4.756	0.040
ln (SSC)	Band 5	0.193	5.485	0.028
ln (SSC)	Band 6	0.219	6.438	0.018
ln (SSC)	Band 7	0.259	8.024	0.009
ln (SSC)	**Band 8**	**** 0.305**	**10.108**	**0.004**
ln (SSC)	Band 9	0.285	9.146	0.006
ln (SSC)	Band 10	0.258	7.998	0.016
Turbidity	Band 6	0.245	7.468	0.012
Turbidity	Band 7	0.303	9.995	0.004
Turbidity	**Band 8**	**** 0.378**	**13.987**	**0.001**
Turbidity	Band 9	** 0.335	11.610	0.002
Turbidity	Band 10	0.218	6.411	0.019

Table by Kin M. Ma (1997)

Table 4.5 – (Cont'd)

Turbidity	**Band 7, Band 8** **–0.386 * (Band 7) + 1.757 * (Band 8) + 28.176**	**** 0.400**	**7.348**	**0.004**
Turbidity	**Band 9, Band 10** **3.983 * (Band 9) – 3.141 * (Band 10) + 49.398**	**** 0.450**	**8.984**	**0.001**
ln(Turbidity)	Band 5	0.209	6.069	0.022
ln(Turbidity)	Band 6	0.261	8.130	0.009
ln(Turbidity)	Band 7	0.314	10.520	0.004
ln(Turbidity)	**Band 8**	****0.377**	**13.928**	**0.001**
ln(Turbidity)	Band 9	0.322	10.912	0.003
ln(Turbidity)	Band 10	0.210	6.124	0.021
ln(Turbidity)	**Band 7, Band 8, Band 9, and Band 10**	****0.488**	**6.709**	**0.001**
ln(Turbidity)	ln (Band 6)	0.208	6.036	0.022
ln(Turbidity)	ln (Band 7)	0.240	7.256	0.013
ln(Turbidity)	ln (Band 8)	0.280	8.932	0.007
ln(Turbidity)	ln (Band 9)	0.234	7.030	0.014
ln(Turbidity)	ln (Band 10)	0.160	4.371	0.048

** yielded relatively high R^2 values

Table by Kin M. Ma (1997)

b. Turbidity

Linear regression analyses generated low correlations with R^2 ranging from 0.20 to 0.30. However, using a logarithmic function the ln(turbidity) and MSS band 8 regression yielded $R^2 = 0.377$ and $p = 0.001$ (Figure 4.14). Through multiple regression, the correlation coefficient of turbidity improved slightly. By regressing Bands 7 and 8 with turbidity the results yielded a correlation relationship of $R^2 = 0.400$ and $p = 0.004$ with a regression equation of:

Turbidity = --0.386 * (Band 7) + 1.757 * (Band 8) + 28.176 (see Table 4.5).

By testing the logarithmic function, the highest correlation coefficient for ln(Turbidity) and MSS Band 8 was similar to the regression of SSC and MSS Band 8, $R^2 = 0.377$ and $p = 0.001$.

Another regression of Bands 9 and 10 and turbidity was significant, $R^2 = 0.450$ and $p = 0.001$, with a regression equation of :

Turbidity = 3.983 * (Band 9) – 3.141 * (Band 10) + 49.398.

An additional multiple regression between ln(Turbidity) and MSS Bands 7, 8, 9, and 10 yielded $R^2 = 0.488$ and $p = 0.001$, F-test = 6.709. The correlation relationship was significant though there is a low F-test and the individual p values for each band were not significant, with approximate p values of 0.20 and 0.50, signifying that MSS Bands 7 and 10 were forced into the regression equation. This caused the overall multiple regression equation of MSS Bands 7, 8, 9, and 10 and ln(Turbidity) to be less significant then the single band regression of ln(Turbidity) and MSS Band 8 already mentioned above.

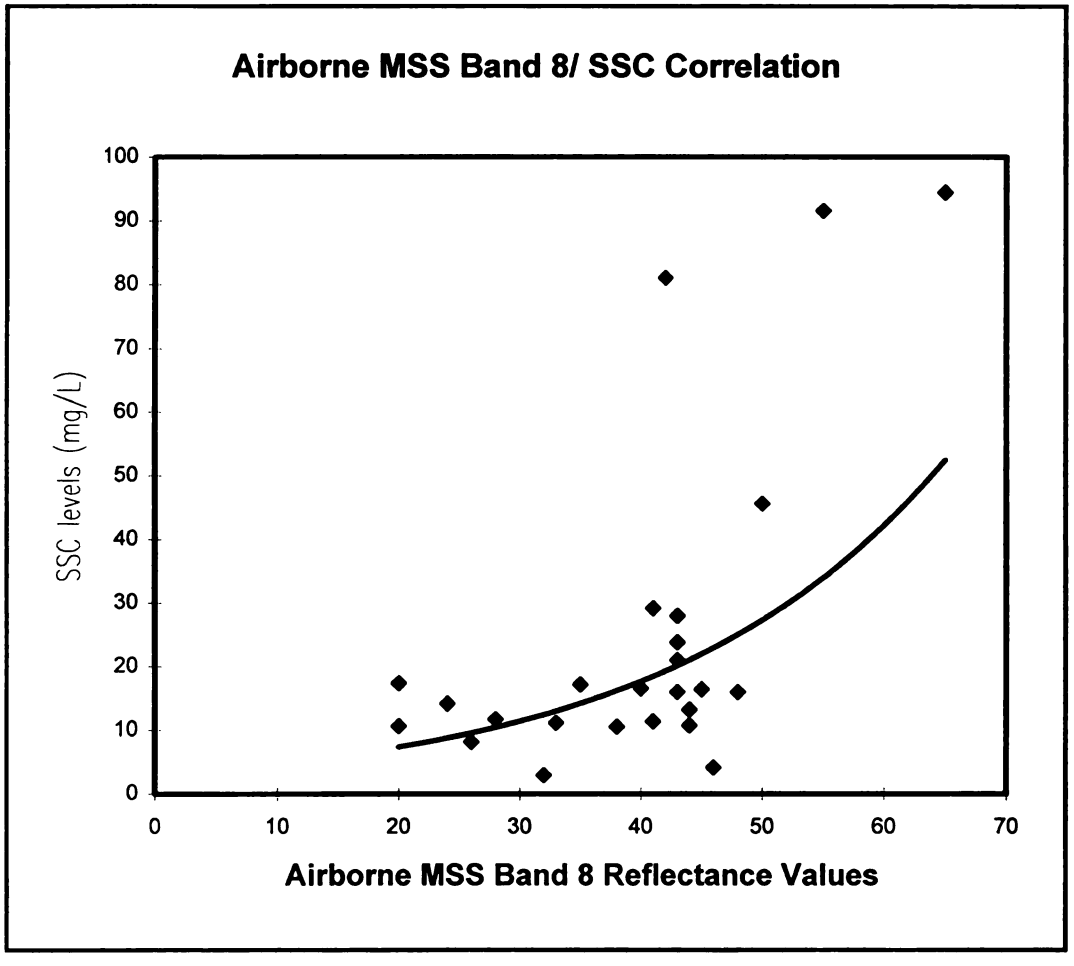

$R^2 = 0.377, p = 0.001$

SSC = 1.495 * (MSS Band_8) -- 34.197

Figure 4.12 – Graph of Correlation between Airborne MSS Band 8 and SSC.

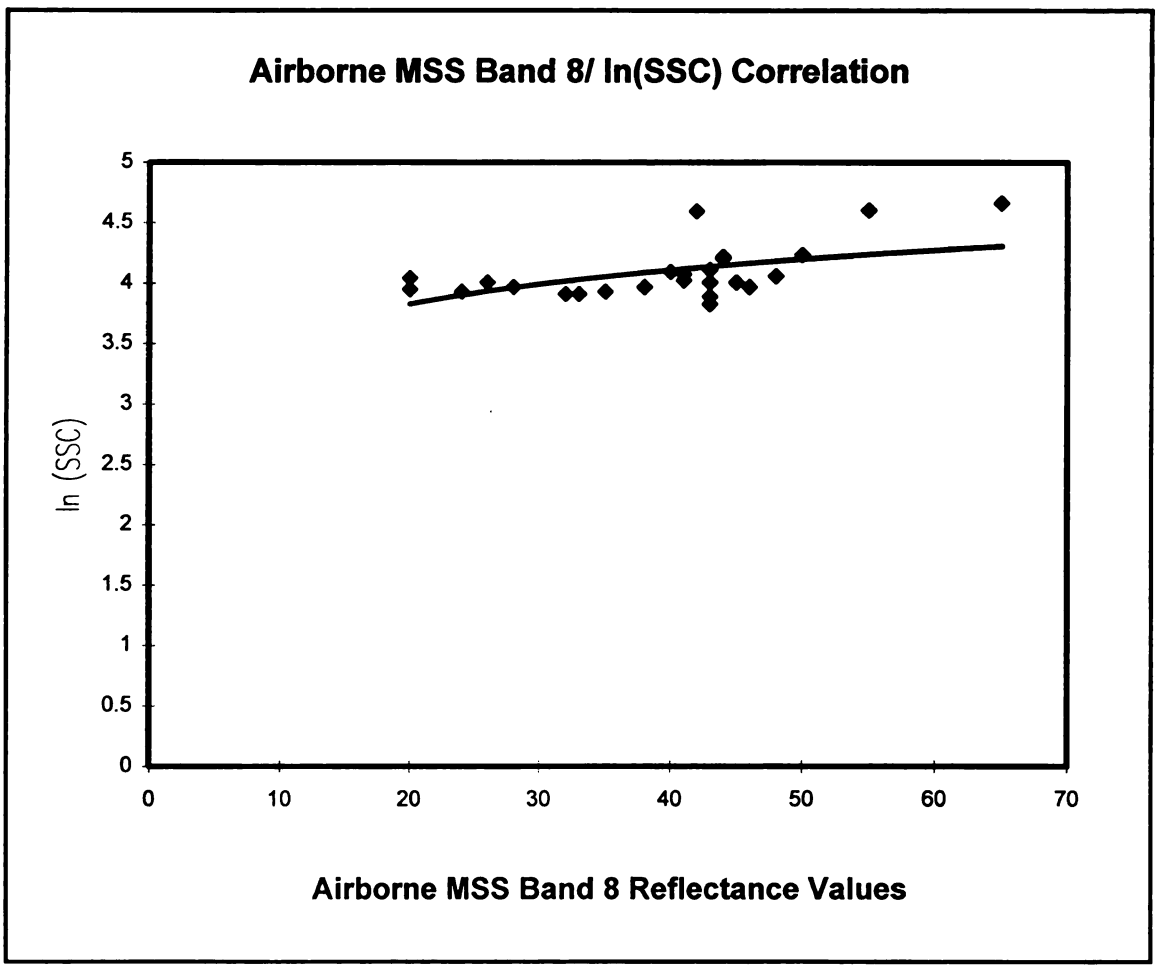

R^2 =0.305, p = 0.004

ln (SSC) = 0.0435 * (MSS Band_8) + 1.136

Figure 4.13 – Graph of Correlation between Airborne MSS Band 8 and ln(SSC).

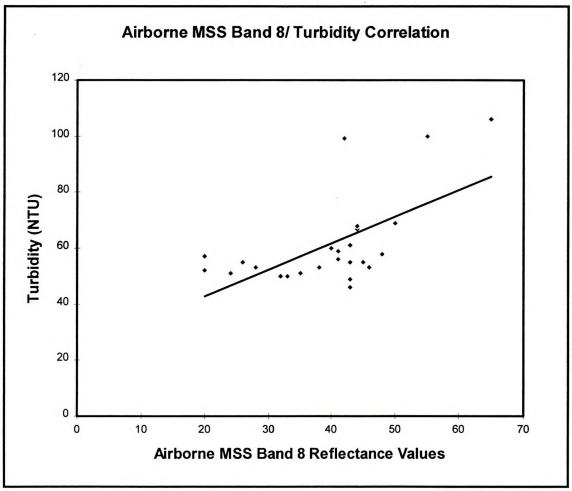

$R^2 = 0.377$ and $p = 0.001$

Turbidity = 0.949 * (MSS Band 8) + 23.790

Figure 4.14 – Graph of Correlation between Airborne MSS Band 8 and Turbidity.

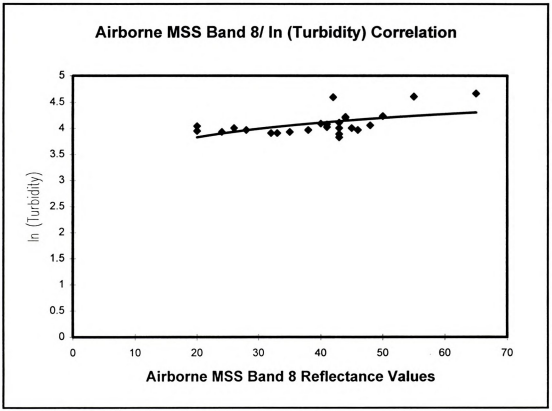

$R^2 = 0.377$ and $p = 0.001$

ln (Turbidity) = 0.0131 * (MSS Band_8) + 3.573

Figure 4.15 – Graph of Correlation between Airborne MSS Band 8 and ln (Turbidity)

C. Discussion

1. Landsat TM image analysis

The linear regression of ln(SSC) and TM Band 4 yielded a significant correlation of $R^2 = 0.571$, though it was not as highly predictive as Braga et al.'s (1993) study yielding a $R^2 = 0.74$ for the correlation between total suspended solids and TM Band 4. Also Khorram and Cheshire's (1985) study regressed the Landsat MSS Bands 4, 5, 6, and 7 complex band ratios and SSC and yielded a $R^2 = 0.64$. These significant correlations support Campbell's (1987) Figure 2.1 showing that high amounts of SSC will reflect more radiant energy in the red and infra-red wavelengths of light, such as Landsat TM Band 4.

The differences in R^2 values may be due to several factors: a) temporal variability of the SSC, b) inaccuracies in the image normalization process, and c) shallowness of the Chilung River body.

a. Temporal Variability in SSC

Water quality data should be temporally matched to the Landsat TM images. However, none of the Landsat TM images were temporally matched to the water quality monitoring dates and times. For example, there was usually a day difference though in the December 11, 1995 image, there is a four day difference in time from the December 7, 1995 water quality monitoring date. During the intervening days between the image date and the testing date, there may have been variations in sediment levels. As Table 1.4, page 11, shows, the SSC levels from 1987 to 1995 greatly varied between high and low values throughout the Chilung River.

b. Inaccuracies in Image Normalization

Since there were an insufficient number of Taiwan EPA SSC water quality test sites from one monthly monitoring sample, three Landsat TM images were normalized to obtain a sufficient number of test data points. During the normalization process, the generated regression equations were very high ranging from $R^2 = 0.874$ to $R^2 = 0.929$, for TM Band 4. There was some loss of reflectance value in the normalization process since the R^2 coefficient did not attain the perfect 1.00. This alteration of reflectance values from the original Landsat TM images may have contributed to lowering the Band 4/SSC R^2 correlations in this study.

c. Shallowness of the River body

The Chilung river is a small, relatively shallow river with many sections less than 5 meters deep (ROC EPA, 1996). Landsat TM reflectance may penetrate the shallow water of the river into the riverbed. Moore's (1978) research showed that solar radiation in the blue-green location, 0.52 μm, can penetrate 2 meters into clear water and all the way up to 20 meters in very, clear water. Therefore, this water penetration may lead to inaccuracies of estimating the amount of SSC from the water quality samples as opposed to estimating the depth of the riverbed. However, this reason may not be very important because the color of the Chilung River was black and very little penetration could occur.

2. Airborne MSS image analysis

The linear and logarithmic relationship generated correlations of $R^2 = 0.377$ for the regression of SSC and MSS Band 8 and $R^2 = 0.284$ for the regression of SSC and MSS Band 7 (see Table 4.5). Curran et al.'s (1987) study yielded significant correlations at similar spectral wavelengths with $R^2 = 0.46$.

Also Miller et al.'s (1994) SSC research in Puerto Rico yielded a very significant $R^2 = 0.85$ for regressing low concentrations of SSC at the 0.63—0.69 μm wavelength sensitivity which would be equivalent to this study's MSS Bands 6 and 7.

The large differences in R^2 values may be due to several factors: a) temporal variability of the SSC, or b) the small 5 meter pixel resolution size combined with Airborne MSS image resampling inaccuracies and errors.

a. Temporal Variability of the SSC

Since the water quality data should temporally match the Airborne MSS image in time and space, there was possible variability of the SSC and turbidity between the day the Airborne MSS image was flown, 4/25/96, and the day that the water quality samples were taken, 4/26/96. As Table 1.4, page 11, shows, the SSC levels from 1987 to 1995 greatly varied between high and low values throughout the Chilung River.

b. Small Pixel Resolution and Resampling Errors

According to Gao and O'Leary (1997), the spatial resolution of the image has a significant role in the accuracy of quantifying SSC in water. Their study showed that a 10 meter pixel resolution produced the best correlation with the SSC data

(R^2 = 0.97) and that as the pixel resolution diminished below 10 meters, the correlation of SSC and band reflectance decreased from R^2 = 0.81 for a 5 meter pixel resolution down to R^2 = 0.75 for a 1 meter pixel resolution image (Gao and O'Leary, 1997). The reasons are because even with the increased accuracy of using the Differential Global Positioning System (DGPS), there may be some variations and errors in rectifying and resampling the aerial image. "Geometric errors can still be present in the rectified image due to the lack of geometric controls over the water surface where no distinct features can be used as GCPs" (Gao and O'Leary, 1997). Also with the small 5 meter pixel resolution, the uncertainty of determining the exact location of the water quality reading is greater, especially if flowing river currents shift the field boat several meters to the right or left during the time that the DGPS reading is being taken.

CHAPTER V

SUMMARY, CONCLUSIONS AND RECOMMENDATIONS

A. SUMMARY

Due to the rapid industrial development within Taiwan over the past 30 years, the accumulated releases of phosphates, nitrates, particulates and heavy metals, associated with industrial development have degraded the water quality of Taiwan's rivers. This caused increases in biological oxygen demand, increases in the suspended sediments concentration (SSC), and decreases in dissolved oxygen. All of these contributing factors have lowered the water quality of the Taiwan river systems. The Chilung River flowing through Taipei City is no exception.

In order to combat the environmental degradation, Taiwan citizens rallied to pressure the Taiwan government to establish the Taiwan Environmental Protection Administration (Taiwan EPA) in 1987. Since 1987, the Taiwan EPA has been sending out monthly field teams to gather water quality monitoring data from the Chilung River and adjoining Tanshui River.

However, this monitoring effort is costly and can only provide specific point samples of water quality monitoring data. Extensive research has been done using remotely sensed images of various water bodies, such as lakes, coastal zones, and large rivers such as the Amazon River (Shimoda et al., 1986; Curran et al., 1987; Mertes, et al., 1994).

This study utilized several Landsat TM images and an Airborne MSS image to determine whether there were significant correlations between the reflectance values and SSC and turbidity levels. Suspended sediments concentration data for the Chilung River were obtained from the monthly Taiwan EPA field data and were temporally matched with three Landsat TM images. The three images were normalized and the reflectance values were transformed into radiance values for increased accuracy of statistical regression analysis.

The Airborne MSS image was flown by the Taiwan Provincial Government, Department of Forestry, Agroforestry Aerial Survey Division, and the field research team collected SSC and turbidity water quality data for over twenty-five sites.

Multi-linear regression analyses between the Landsat TM radiance values and SSC showed significant correlations between TM Band 4, the near-infrared band, and suspended sediment concentrations (SSC) with $R^2 = 0.444$, $p = 0.009$ (see Table 4.4). Utilizing the logarithmic function, the regression of the ln(SSC) dependent variable and the Band 4 radiance values yielded the highest significant single band correlational relationship, $R^2 = 0.574$, $p = 0.002$, with a regression equation: ln(SSC) = 0.157*(Band 4) + 2.582. Also, the (Band 4/Band 2) ratio regression against ln(SSC) yielded a high correlation, $R^2 = 0.66$, $p = 0.001$ (see Figure 4.8).

Multi-linear regression analyses of the Airborne MSS reflectance values and SSC yielded significant correlations between MSS Band 8 and 9, the near infrared bands (see Table 2.1). Utilizing logarithmic function analysis, the regression of ln(turbidity) and MSS Band 8 was significantly correlated, $R^2 = 0.377$, $p = 0.001$ (see Figure 4.12).

B. CONCLUSIONS

The conclusions of this study are presented as responses to the following research questions:

Research Questions

1) Can the water quality of the entire Chilung River be efficiently assessed using remotely sensed images and not just areas from which water quality point samples were collected?

It is efficient to use Landsat TM images for monitoring the suspended sediments of the Chilung River because the Landsat-5 satellite continues to pass over the Taipei area at regular 16-day intervals, and significant correlations between SSC and TM Band 4 have been found. However, since the Chilung River is relatively narrow at the NanHu bridge, some locations may only have several pixels which span the width of the river and not be very accurate in estimating SSC levels of the Chilung River, since these 900 sq. meter edge pixels of the Chilung River may be mixed with the adjoining land features, such as the eastern region of the research area.

The finer resolution of the Airborne MSS image, 5 meter pixel resolution, may help the water quality assessment problem. However, the use of Airborne MSS would be too expensive for use in periodic monitoring since flying and processing one Airborne MSS image costs over US$10,000 in Taiwan. Also, there are inaccuracies of using an image with very fine resolution for water quality assessment, and of ground truthing in a aqueous environment where there are no good landmarks for resampling the MSS image (Gao and O'Leary, 1997).

2) Is there a significant correlation between the reflectance values of the remotely sensed images with the collected water quality data of the Chilung River?

As stated above, there are significant correlations between Landsat TM radiance values and TM Band 4, the infrared band. The Airborne MSS reflectance bands 9 and 10, the infrared bands, also have been significantly correlated with SSC.

These remotely sensed images can be used to periodically monitor the SSC and turbidity levels of the Chilung River, though periodic field water quality testing is still needed, since the Landsat TM data showed a large variability of SSC values at several sites in which the reflectance values were the same. e.g. SSC values of 39.3, 19.5 and 18.0 mg/L in the December 1995 TM image yielded the same reflectance value of "5" (see Table 3.1, page 23).

3) Which type of remotely sensed images, Landsat TM or Airborne MSS, yield better correlations between Chilung River water quality values and their respective reflectance values?

As the correlation results show, Landsat TM Band 4 and ln(SSC) yielded the highest $R^2 = 0.571$, while the equivalent Airborne MSS spectral wavelengths, Bands 8 and 9, yielded R^2 of 0.38 and 0.37. Landsat TM holds promise to be a better predictor of SSC in this study for periodical water quality monitoring. Airborne MSS reflectance values yielded significant correlations, though there may be some problems of positional accuracy with its small 5 meter pixel resolution. These problems were explained in detail in the Chapter 4 discussion section.

C. RECOMMENDATIONS

Recommendations for Scholars

More efforts need to be made to coordinate simultaneous flying of the image and conducting the field water quality testing since this will eliminate the potential variability in the water quality parameters between the date and time the remotely sensed image is flown and the suspended sediment or turbidity water quality readings.

Since Gao and O'Leary (1997) suggested that a pixel resolution of 10 meters would be the ideal resolution for obtaining the best R^2 correlation between SSC and airborne remotely sensed data, further research should seek to find a remote sensor having a 10 meter pixel resolution which matches the band spectral sensitivity of the Landsat TM sensor, or fly the Airborne MSS image at a higher altitude to increase the pixel resolution to 10 meters.

Recommendations for the Taiwan EPA

Since there were significant correlations between suspended sediment concentrations and Landsat TM radiance values, Landsat TM images can be used to supplement the Taiwan EPA's water quality monthly monitoring program since images can be obtained at 16-day periodic intervals.

If the number of monthly water quality monitoring data points were increased, there would be a more representative distribution of the SSC within the Chilung River and increased likelihood of more accurately predicting the SSC levels

in the Chilung River when regressed against the radiance values of the Landsat TM images.

Also, several monthly water quality monitoring dates could be planned to coincide with the Landsat TM flight date(s) over the Taipei region to test whether more highly significant correlations will be generated when the variability between the remotely sensed image flight date and the test monitoring date is eliminated.

The Taiwan EPA may consider using this method of using Landsat TM images to help monitor SSC and turbidity of other less accessible Taiwan rivers and coastline areas since the Landsat TM sensor can easily fly over any region of Taiwan island.

Recommendations for other governments

Since significant correlations could be established between SSCs and Landsat TM data for a small, shallow Chilung River in Taipei, Taiwan, other governments can also attempt to obtain Landsat TM images to help monitor the suspended sediments concentration in medium to small rivers in areas of difficult access.

APPENDICES

APPENDIX A

MAP OF EAST ASIA

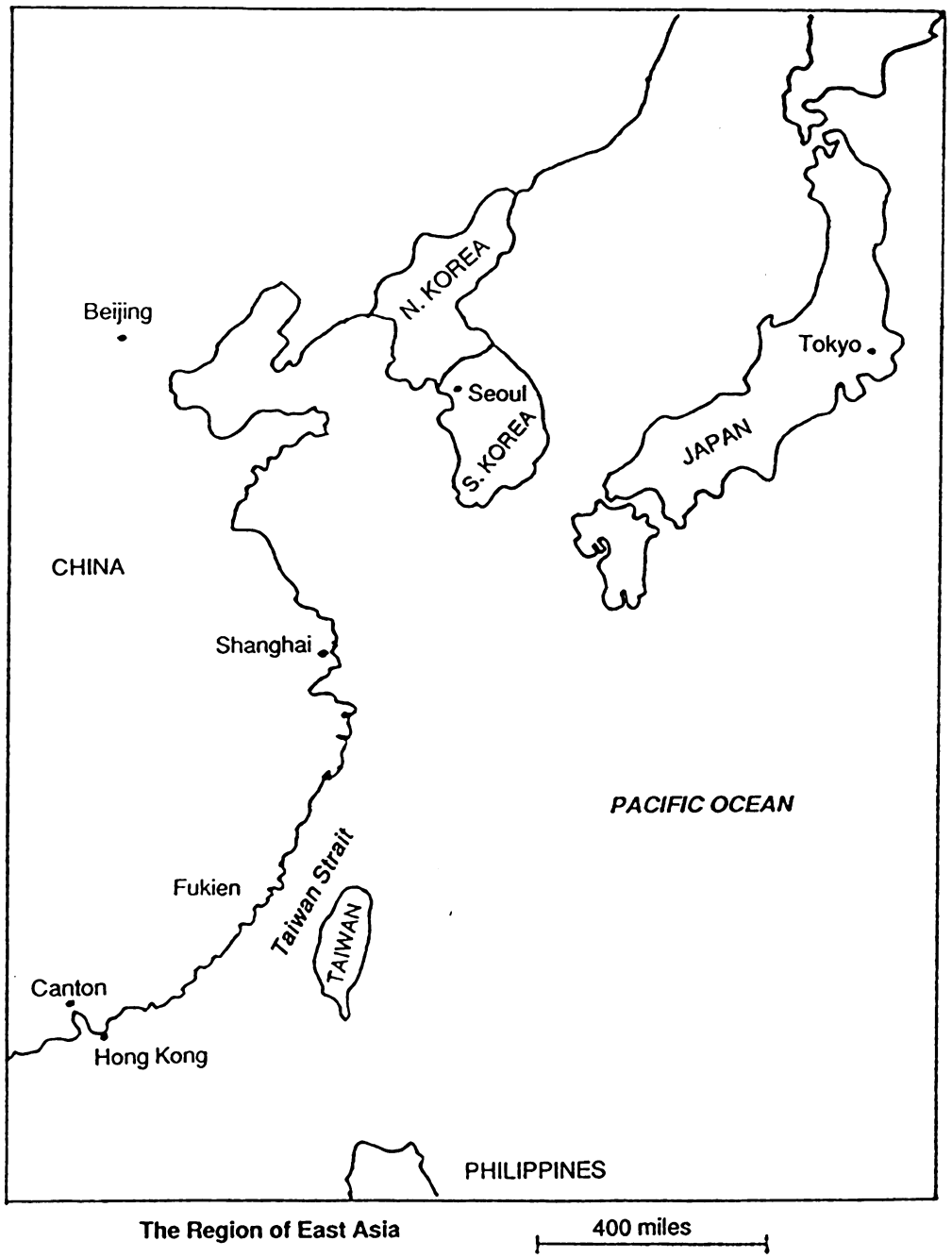

Source: James Reardon-Anderson, *Pollution, Politics and Foreign Investment in Taiwan,* (M.E. Sharpe, Inc., Armonk, NY, 1992), p. xii.

APPENDIX B

NORTHERN TAIWAN, TAIPEI REGION AND SURROUNDING CITIES

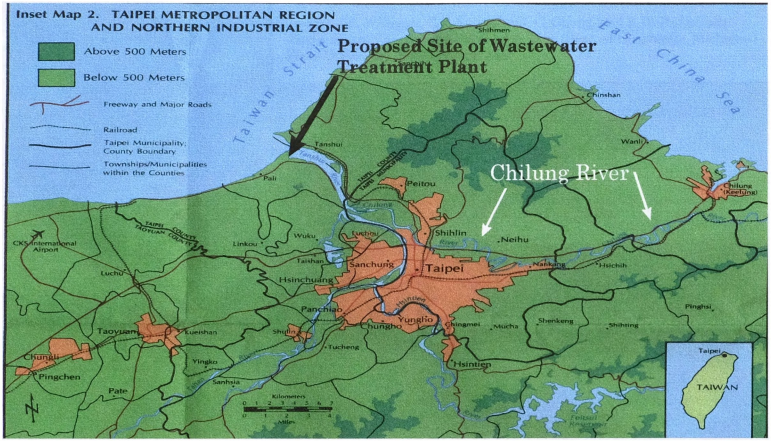

Source: J.F. Williams, C.F. Sutherland, C. Chang, and R.D. Tiefenbach. *Taipei Basin, Taiwan Land Use*, 1983, Map (Dept. of Geography, Michigan State University, East Lansing, MI).

APPENDIX C

EASTERN CHILUNG RIVER, TAIPEI, TAIWAN

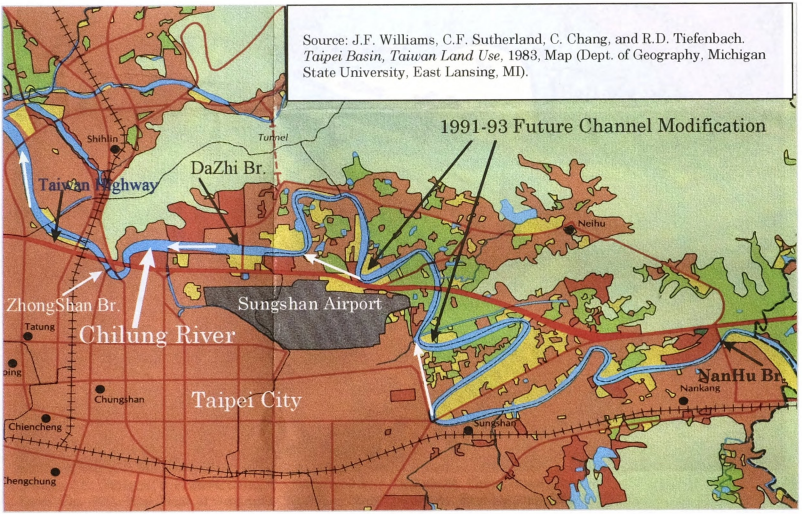

APPENDIX D

WESTERN CHILUNG RIVER, TAIPEI, TAIWAN

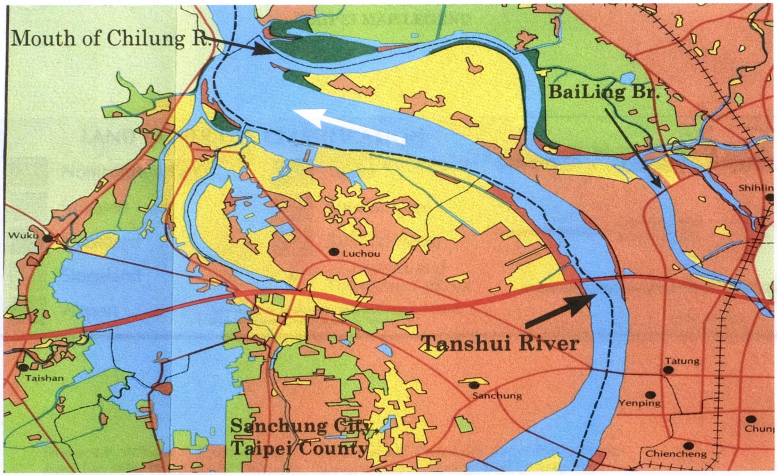

Source: J.F. Williams, C.F. Sutherland, C. Chang, and R.D. Tiefenbach. *Taipei Basin, Taiwan Land Use*, 1983, Map (Dept. of Geography, Michigan State University, East Lansing, MI).

APPENDIX E

TAIPEI MAP LEGEND

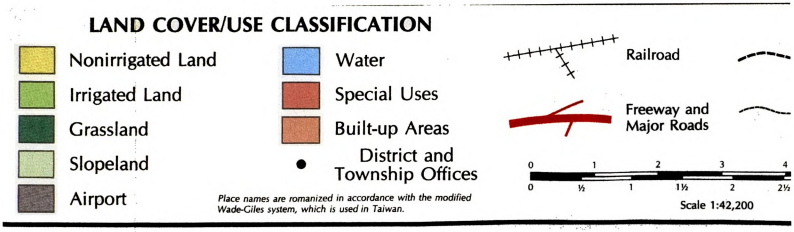

Source: J.F. Williams, C.F. Sutherland, C. Chang, and R.D. Tiefenbach. *Taipei Basin, Taiwan Land Use*, 1983, Map (Dept. of Geography, Michigan State University, East Lansing, MI).

BIBLIOGRAPHY

BIBLIOGRAPHY

Alföldi, T.T. (1982). Remote sensing for water quality monitoring. In *Remote Sensing for Resource Management.* (Johannsen, C.J. and J.L. Sanders, Eds.), Soil Conservation Society of America, Ankeny, Iowa, pp. 317-327.

Braga, C.Z.F., A.W. Setzer, and L.D. de Lacerda. (1993). Water quality assessment with simultaneous Landsat-5 TM data at Guanabara Bay, Rio de Janeiro, Brazil. *Remote Sensing of Environment,* 45(1): 95-106.

Campbell, J.B. (1987). *Introduction to Remote Sensing.* The Guilford Press, New York, NY, pp. 283-287, 404-433.

Clark, W.A.V. and P.L. Hosking. (1986). *Statistical Methods for Geographers.* John Wiley & Sons, Inc., New York, NY, pp. 334-349.

Curran, P.J., J.D. Hansom, S.E. Plummer, and M.I. Pedley. (1987). Multispectral remote sensing of nearshore suspended sediments: a pilot study. *International Journal of Remote Sensing,* 8(1): 103-112.

Dzurik, A.A. (1990). *Water Resources Planning.* Rowman & Littlefield Publishers, Inc., Savage, Maryland, 318 pp.

Gao, J. and S.M. O'Leary. (1997). The role of spatial resolution in quantifying SSC from Airborne remotely sensed data. *Photogrammetric Engineering and Remote Sensing,* 63(3): 267-271.

Han, L. and D.C. Rundquist. (1994). The response of both surface reflectance and the underwater light field to various levels of suspended sediments: Preliminary results. *Photogrammetric Engineering and Remote Sensing,* 60(12): 1463-1471.

Jensen, J.R., K. Rutchey, M.S. Koch, and S. Narumalani. (1995). Inland wetland change detection in the Everglades water conservation area 2A using a time series of normalized remotely sensed data. *Photogrammetric Engineering and Remote Sensing,* 61(2): 199-209.

Khorram, S. and H. Cheshire. (1985). Remote sensing of water quality in the Neuse River Estuary, North Carolina. *Photogrammetric Engineering and Remote Sensing,* 51(3): 329-341.

Kirk, J.T.O. (1989). The upwelling light stream in natural waters. *Limnology and Oceanography*, 34: 1410-1425.

Lavery, P., C. Pattiaratchi, A. Wyllie, and P. Hick (1993). Water quality monitoring in estuarine waters using the Landsat Thematic Mapper. *Remote Sensing of Environment*, 46(3): 268-280.

Liedtke, J., A. Roberts, and J. Luternauer. (1995). Practical remote sensing of suspended sediment concentration. *Photogrammetric Engineering and Remote Sensing*, 61(2): 167-175.

Lillesand, T.M. and R.W. Kiefer. (1987). *Remote sensing and image interpretation.* Second edition. John Wiley & Sons, Inc., New York, NY, pp. 450-466.

Lillesand, T.M. and R.W. Kiefer. (1994). *Remote sensing and image interpretation.* Third edition. John Wiley & Sons, Inc., New York, NY, pp. 202-214, 462-480, 524-541.

Lusch, D.P. (1996). *Introduction to GPS: The Global Positioning System.* Manual published for the Center for Remote Sensing, Dept. of Geography, and Institute for Water Research, Michigan State University, East Lansing, MI, 28 pp.

Mertes, L.A.K., M.O. Smith, and J.B. Adams. (1993). Estimating suspended sediment concentrations in surface waters of the Amazon River wetlands from Landsat images. *Remote Sensing of Environment*, 43(3): 281-301.

Miller, R.L., J.F. Cruise, E. Otero, J.M. Lopez. (1994). Monitoring suspended particulate matter in Puerto Rico: Field measurements and remote sensing. *Water Resources Bulletin*, 30(2): 271-282.

Moore, G.K. (1978). Satellite surveillance of physical water quality characteristics. In *Proceedings of the Twelfth International Symposium on Remote Sensing of Environmen, Volume 1, April 20-26, 1978.* Environmental Research Institute of Michigan, Ann Arbor, MI, pp. 445-462.

Pattiaratchi, C.B., P. Lavery, A. Wyllie, and P. Hick. (1994). Estimates of water quality in coastal waters using multi-date Landsat Thematic Mapper data. *International Journal of Remote Sensing*, 15(8): 1571-1584.

Reardon-Anderson, J. (1982). *Pollution, Politics and Foreign Investment in Taiwan.* M.E. Sharpe, Inc., Armonk, NY, p. xii.

Republic of China, Environmental Protection Administration. (1989). *Report on the Plan to Treat the flow of Wastewater from the Chilung River.* December 1989, Taipei, Taiwan (in Chinese).

Republic of China, Environmental Protection Administration. (1994a). *1993 State of the Environment, Taiwan, Republic of China.* (Lung-Sheng Chang, Ed.), Taipei, Taiwan, 473 pp.

Republic of China, Environmental Protection Administration. (1994b). *Case Report on the Plan to Treat the Pollution of the Tanshui River.* June, 1994, Taipei, Taiwan (in Chinese).

Republic of China, Environmental Protection Administration. (1996). *The Application of Remote Sensing Technique on the Study of Environmental Pollution Monitoring.* Prepared by the Center for Geographic Information Systems Research, Feng Chia University, June, 1996, Taichung, Taiwan, 163 pp., (in Chinese).

Republic of China, National Weather Bureau. (1988- 1996). Monthly weather reports from January 1987 to December 1995 (in Chinese).

Rimmer, J.C., M.B. Collins, and C.B. Pattiaratchi. (1987). Mapping of water quality in coastal waters using airborne thematic mapper data. *International Journal of Remote Sensing,* 8(1): 85-102.

Ritchie, J.C., C.M. Cooper, and F.R. Schiebe. (1990). The relationship of MSS and TM data with suspended sediments, chlorophyll, and temperature in Moon Lake, Mississippi. *Remote Sensing of Environment,* 33: 137-148.

Shimoda, H., M. Etaya, T. Sakata, L. Goda, and K. Stelczer. (1986). Water quality monitoring of Lake Balaton using Landsat MSS data. Seventh International Symposium on Remote Sensing for Resources Development and Environmental Management. (Damen, M.C.J., G.S. Smit, and H.T. Verstappen, Eds.), August 1986, Enschede, Netherlands, pp. 765-770.

Welch, R., M.M. Remillard, and R.B. Slack. (1988). Remote sensing and geographic information system techniques for aquatic resource evaluation. *Photogrammetric Engineering and Remote Sensing,* 54(2): 177-185.